The Transmission and Transformation of Baroclinic Rossby Waves by Topography*

J. PEDLOSKY
Woods Hole Oceanographic Institution, Woods Hole, Massachusetts

(Manuscript received 6 October 1999, in final form 8 February 2000)

ABSTRACT

The transmission of westward propagating baroclinic Rossby waves incident on a gappy meridional barrier is studied in the context of the two-layer, quasigeostrophic model. The meridional barrier models the presence of very steep topography such as the midocean ridge system or extensive island arcs.

The nature of the transmission depends strongly on the nature of the gaps in the meridional barrier. If the gaps extend throughout the depth of the fluid, the Rossby waves propagate through the barrier, as a consequence of Kelvin's theorem, with no change in vertical structure. On the other hand, if the gaps in the barrier are partial and extend only over a single layer, there is a significant transformation of the vertical structure of the wave field as it traverses the barrier. In particular, waves of baroclinic vertical structure in the model are transformed on the western side of the barrier into barotropic waves that radiate from the segment of the barrier between two such gaps. Such segments act as antennae radiating barotropic energy into the western subbasin. It is suggested that recent observations of signal enhancement of Rossby waves at the midocean ridge system in the Pacific may be related to such transformation of wave structure.

The problems of free waves and forced waves in open regions and normal modes in closed basins are described.

1. Introduction

Recent observations of planetary scale oceanic Rossby waves have established the ability of these large scale waves to propagate great zonal distances. The study of Chelton and Schlax (1996, hereafter CS) in particular emphasized the apparent role of the strong topography of the midocean ridge system in affecting the propagation of the waves. Of special interest, CS describe the apparent amplification of the first (vertical) baroclinic mode in the region west of the ridge system with respect to the signal in the eastern Pacific and suggest that the topography itself may be a source for the westward propagating mode (see also Zang and Wunsch 1999). Since topography, on its own, cannot be a source of wave energy, the implication is that some interaction of the preexisting oceanic motion field with the topography is central to the explanation of this intriguing observation.

Previous theoretical work on the interaction of Rossby waves and topography, for example, considered essentially weak topography within the quasigeostrophic context. Most of these studies have, in addition, dealt with the problem in the context of a barotropic model, for example the work of Anderson and Killworth (1977), Barnier (1984), and Matano (1995), and hence were not in a position to discuss the possibility of barotropic to baroclinic conversion by interaction with topography. Wang and Koblinsky (1994) discuss a two-layer quasigeostrophic model with very weak topography in the lower layer and do find evidence for such conversion. However, as the amplitude of the ridge in their model becomes large, incident wave energy from the east becomes increasingly reflected by the barrier denying passage of energy into the western sub-basin.

Pedlosky and Spall (1999, hereafter PS) have argued that such steep topography might better be represented at lowest order by vertical barriers, broken open in places to represent faults and gaps in the oceanic ridge system. Such barriers, with their gaps, introduce islandlike segments to the topographic features, and PS have shown that such island segments act as antennae radiating westward the energy impinging on the barrier from the east in such a way that the barrier becomes nearly transparent to the passage of the Rossby wave. To emphasize this point, PS examined the Rossby normal modes of a homogeneous fluid in a basin which was nearly divided in two by a barrier that contained only two very small gaps. They showed that the application of Kelvin's circulation theorem to the interval of the barrier between the two gaps implied a strong transmission of energy past the barrier, whereas a single gap alone, eliminating the islandlike character of the ridge segment, would allow only a very small transmission

*Woods Hole Oceanographic Institution Contribution Number 10106.

Corresponding author address: Dr. Joseph Pedlosky, Dept. of Physical Oceanography, Woods Hole Oceanographic Institution, Clark 363 MS #21, Woods Hole, MA 02543.
E-mail: jpedlosky@whoi.edu

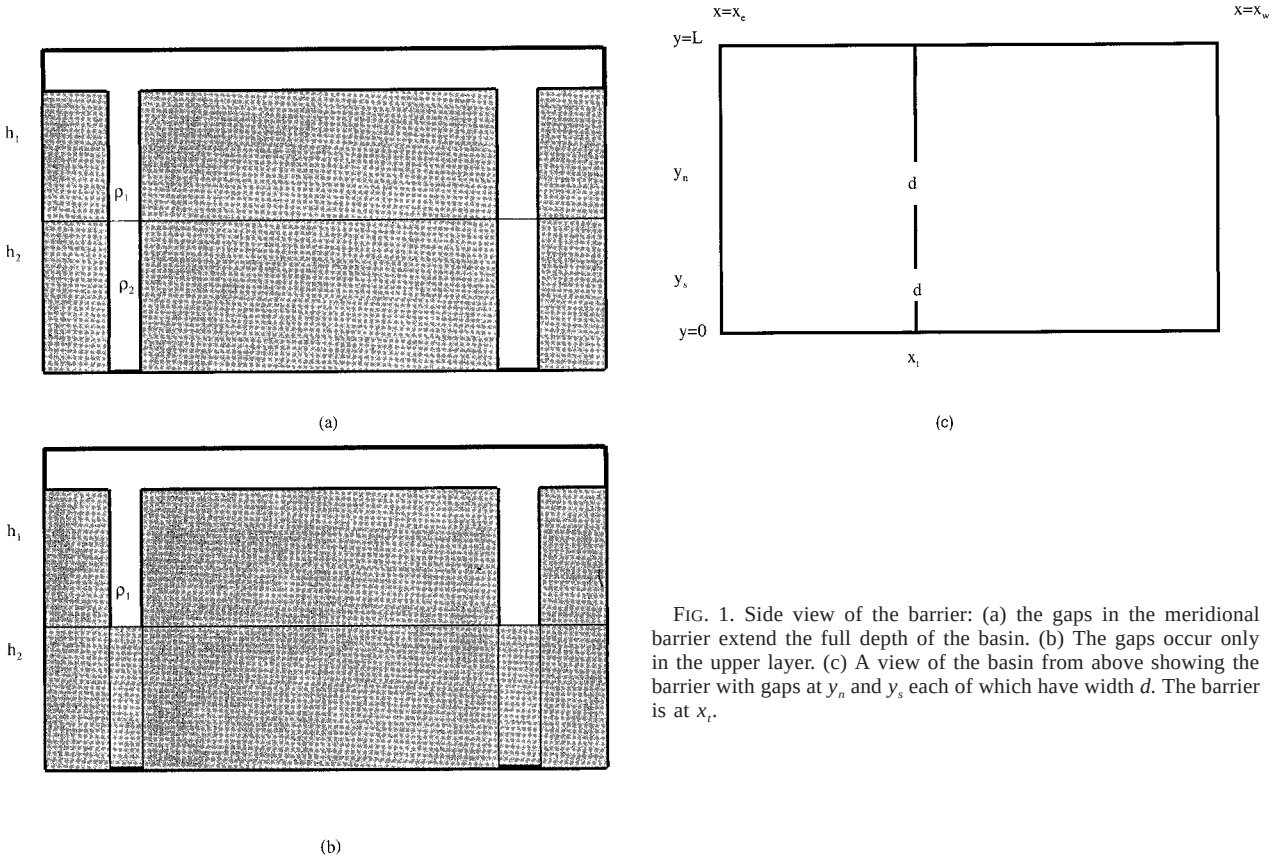

FIG. 1. Side view of the barrier: (a) the gaps in the meridional barrier extend the full depth of the basin. (b) The gaps occur only in the upper layer. (c) A view of the basin from above showing the barrier with gaps at y_n and y_s each of which have width d. The barrier is at x_t.

of wave amplitude, proportional to the ratio of the gap width to the wavelength of the incident wave. Indeed, earlier work by McKee (1972) shows that the magnitude of the transmitted streamfunction would be of the order of the square of this ratio. This antenna effect, absent in previous theoretical studies, forms an essential element of the present study.

In the present paper the theory of the transmission of Rossby waves past such barriers is studied in the context of a baroclinic, two-layer quasigeostrophic model. While highly idealized, the model allows us to discuss not only the transmission of baroclinic wave energy but also the *transformation* of the vertical structure of the wave signal as it passes over and through the topography. The model itself is too simple to mimic precisely the physical situation represented by the measurements of CS. However, the basic issue of the transformation of the wave energy is suggestive of an important role for topography in acting as a source for wave energy of a different vertical structure, that is, more barotropic, than that of the incident wave energy and so, possibly, of a source of energy more easily observable in the satellite altimeter data used by CS. The ease of transmission of this energy is related to the islandlike character of the barrier segments and so also has implications for the transmission of wave energy through island arc chains.

In section 2 the basic two-layer model is described. In this paper both forced and free motions are studied. The forcing that is imposed has both baroclinic and barotropic components and is meant to mimic other physical processes than the linear Rossby wave dynamics described explicitly by the model. These might be potential vorticity sources such as wind forcing or internal processes such as localized eddy fluxes of potential vorticity.

The topography that is considered consists of a long, slender meridional barrier. Its profile is shown in Fig. 1. The barrier generally extends into both layers and rises high enough into the upper layer to effectively completely block the zonal motion there as a consequence of the Taylor–Proudman theorem. Gaps in the barrier allow narrow regions of communication across the barrier. The gaps studied here are of two types. In Fig. 1a the gaps are shown to extend to the full depth of the fluid. As will be seen below, such deep gaps allow the transmission of wave energy with no alteration of the vertical structure of the wave signal. The case shown in Fig. 1b is of more interest. In this case the gaps are partial, that is, they extend only partially through the total depth. For simplicity, in this model, we suppose that the upper layer contains the gaps while the lower layer is completely blocked.

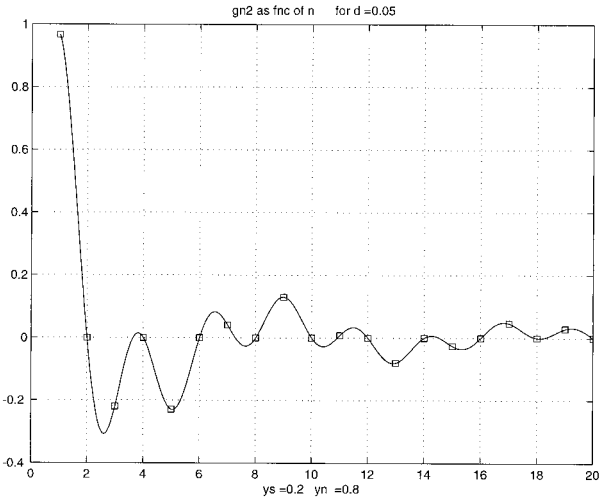

FIG. 2. The function g_{n2} as a function of n for the case $y_s = 0.2$, $y_n = 0.8$, and $d = 0.05$. The function is defined for only integer values of n as shown by the squares, the solid line is added to aid the eye in sensing the it behavior with increasing *n*.

For the island segment between the two gaps, Kelvin's theorem provides an important constraint that is central to understanding the process of wave transmission. In addition, *if the basin is closed at its zonal extremes*, that is, if the wave reflection from the eastern and western boundaries of the basin is considered, a mass conservation integral (McWilliams 1977; Flierl 1977) must also be considered for the baroclinic portion of the motion. Both of these integral constraints represent the response within the quasigeostrophic dynamics of the passage around the perimeter of the basin and around the island segment of the barrier of fast Kelvin waves. These Kelvin waves set up boundary forcing terms that produce Rossby wave radiation in addition to the direct internal forcing represented within the quasigeostrophic potential vorticity equation.

Section 3 describes the interaction of an incident wave from the east with the topography represented by the barrier in Fig. 1 in both the full and partial gap cases. For completeness, the simple problem of such an interaction with a barrier that exists *only* in the lower layer is also considered as a touchstone example for the more complicated cases to be described. This simple case nevertheless contains some important aspects of the transformational character of the topography on the wave signal. Section 4 describes the forced response of the fluid to periodic but spatially localized forcing in the eastern basin and the propagation of the signal beyond the barrier. The varying character of the transmitted wave as a function of stratification and frequency is emphasized. In particular, when the deformation radius is small compared to the basin scale, it is shown that the presence of even a small amount of potential vorticity damping leads to a dominance of the barotropic signal west of the barrier.

In section 5 the basin is closed at its eastern and western ends and the normal modes are described by examining the resonance response of the closed basin to periodic forcing. Both the full gap and partial gap geometries are considered, and in the latter case the normal modes consist of mixtures of barotropic and baroclinic vertical modes. Finally in section 6 we sum up the results and speculate on their application to the observations described above.

2. The model

We consider the quasigeostrophic two-layer model (Pedlosky 1987). For the present purposes only the linearized form of the equations on the beta plane are considered. The equations may be written in the nondimensional form:

$$\left(\frac{\partial}{\partial t} + \kappa\right)[\nabla^2\psi_n + F_n(-1)^n(\psi_1 - \psi_2)] + \frac{\partial \psi_n}{\partial x} = \frac{w_e}{h_n}\delta_{n1} + (-1)^n\frac{w_*}{h_n}, \qquad n = 1, 2. \tag{2.1}$$

The dependent variables carry subscripts 1 and 2 for variables in the upper and lower layers respectively.

In (2.1) time has been scaled with $(\beta L)^{-1}$, where L is the north–south extent of the region, and κ is a coefficient for the decay of potential vorticity perturbation; the timescale for decay also being scaled with βL. For simplicity I have chosen a dissipation representation in which the decay of potential vorticity follows a simple Rayleigh damping law with coefficient κ. Of course, other forms are possible, such as a diffusion of potential vorticity, but the present form is advantageous for its simplicity and similar in its results.

The rotational Froude numbers are

$$F_n = \frac{f_o^2 L^2}{g' H_n}, \tag{2.2}$$

where the undisturbed layer thickness of each layer is H_n and g' is the reduced gravity of the interface. The stream function has been scaled with an amplitude

$$\frac{f_o L W_o}{\beta H},$$

where W_o is the characteristic magnitude of the vertical velocity at the top of the upper layer. Its form is given by w_e and can be thought of either as an Ekman pumping velocity due to the wind stress, if the model is considered a full ocean model, or as the vertical motion from the abyss into the thermocline if the model is considered as dealing with only the abyss. There is a cross-isopycnal velocity w_* at the interface between the two layers. These vertical velocities in the model act as potential vorticity (PV) sources for the two layers and stand in for any process we wish to specify that yields a source of potential vorticity such as eddy fluxes of PV. The fractional layer thicknesses, $h_n = H_n/H$ where

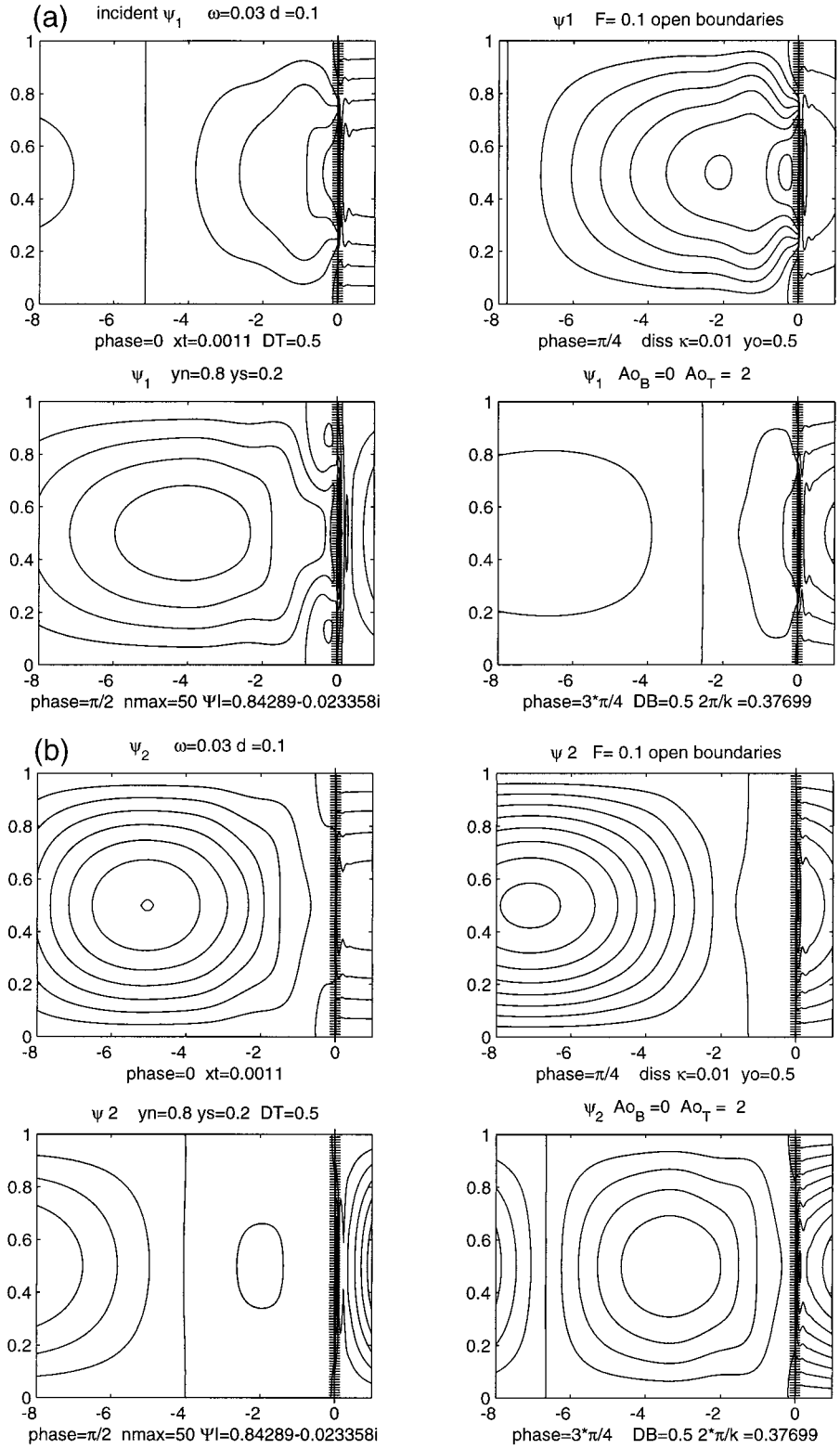

FIG. 3. The transmission of an incident wave in the case of large deformation radius (small F). Here $\kappa = 0.01$, $d = 0.1$, $y_s = 0.2$, $y_n = 0.8$, and the incident wave to the right of the barrier is purely baroclinic. The frequency of the wave is 0.03. Gaps in the barrier exist only in the upper layer. The barrier is indicated by the line of + signs. (a) Snapshots at four moments during the wave period of the upper-layer wave showing the wave penetrating the barrier. (b) As in (a), but for the lower layer. (c) The absolute value of the wave amplitude of the upper layer with selected contours shown. (d) As in (c) but for the lower layer.

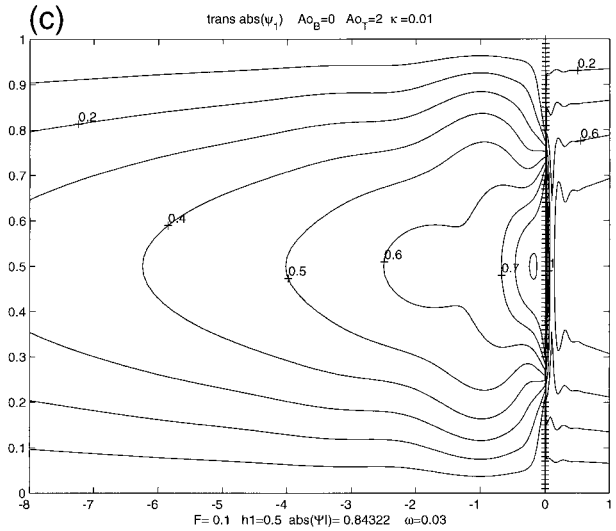

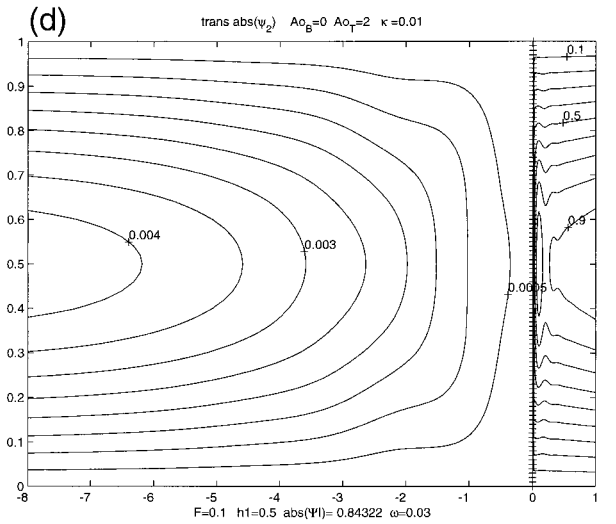

FIG. 3. (*Continued*)

$H = H_1 + H_2$. The Kronecker delta function in (2.1) limits the influence of w_e to the upper layer.

The boundary conditions for (2.1) are as follows.

At all solid boundaries the streamfunction must be independent of position along the boundary but may be (and usually is) a function of time. Since only periodic motions will be considered in this paper, the time dependence of the streamfunction will be of the form $e^{i\omega t}$.

Thus in the upper layer, along the outer perimeter of the basin and along the extensions of that perimeter at the longitude of the ridge,

$$\psi_1 = \Psi_1 e^{i\omega t}, \tag{2.3a}$$

while along the segment of the ridge that is isolated from the basin's perimeter,

$$\psi_1 = \Psi_{I1} e^{i\omega t}, \tag{2.3b}$$

where the I subscript reminds us that it applies to the islandlike segment.

If the gaps in the barrier extend to the bottom, that is, through the second layer, a similar condition holds there. Thus in the case where Fig. 1a is pertinent,

$$\psi_2 = \Psi_2 e^{i\omega t} \tag{2.3c}$$

on the outer boundary of the basin and its connecting peninsulas, while on the islandlike segment in layer 2,

$$\psi_2 = \Psi_{I2} e^{i\omega t}. \tag{2.3d}$$

All four of these constants may differ from each other. The difference between $\Psi_{ln} - \Psi_n$ represents the amplitude of the flux of fluid in the nth layer flowing through the gap. Of course, this will generally vary from layer to layer.

On the other hand if the situation of Fig. 1b applies, the lower layer is divided into two geographically separate subbasins (although they can be linked dynamically) and there is no reason why the streamfunction on the boundary need be the same in each subbasin.

Thus in that case, in the right-hand subbasin we will have

$$\psi_2 = \Psi_2^R e^{i\omega t} \tag{2.3e}$$

on all sides of the eastern subbasin, including the unbroken ridge, while in the western, left-hand-side basin,

$$\psi_2 = \Psi_2^L e^{i\omega t} \tag{2.3f}$$

on the boundaries.

One of these constants can be arbitrarily chosen to be zero, and in the following we will take $\Psi_1 = 0$.

The potential vorticity equation (2.1) must be supplemented by several integral constraints.

The conservation of circulation, when applied to the islandlike segment of the ridge in each layer yields the condition,

$$\left(\frac{\partial}{\partial t} + \kappa\right) \oint_{C_n} \mathbf{u}_n \cdot \hat{t}\, ds = 0, \qquad n = 1, 2, \tag{2.4}$$

where $\hat{t}$ is the tangent vector to the segment and C_n is the contour around the segment. The constraint (2.4) applies in each layer in the case shown in Fig. 1a while, for the case of partial barriers as in Fig. 1b, the constraint applies to only the upper layer.

When, as in the present case, the island segment is idealized as being of infinitesimal width and the motion is either periodic in time or started from rest, (2.4) reduces to the statement that the integral of the meridional velocity along the length of the segment must be the same on both sides of the segment.

As discussed by McWilliams (1977) an additional constraint results from the condition of mass conservation. This is a constraint on the interface between the two layers and can be obtained by integrating the equation for mass conservation over a closed domain in the lower layer to yield

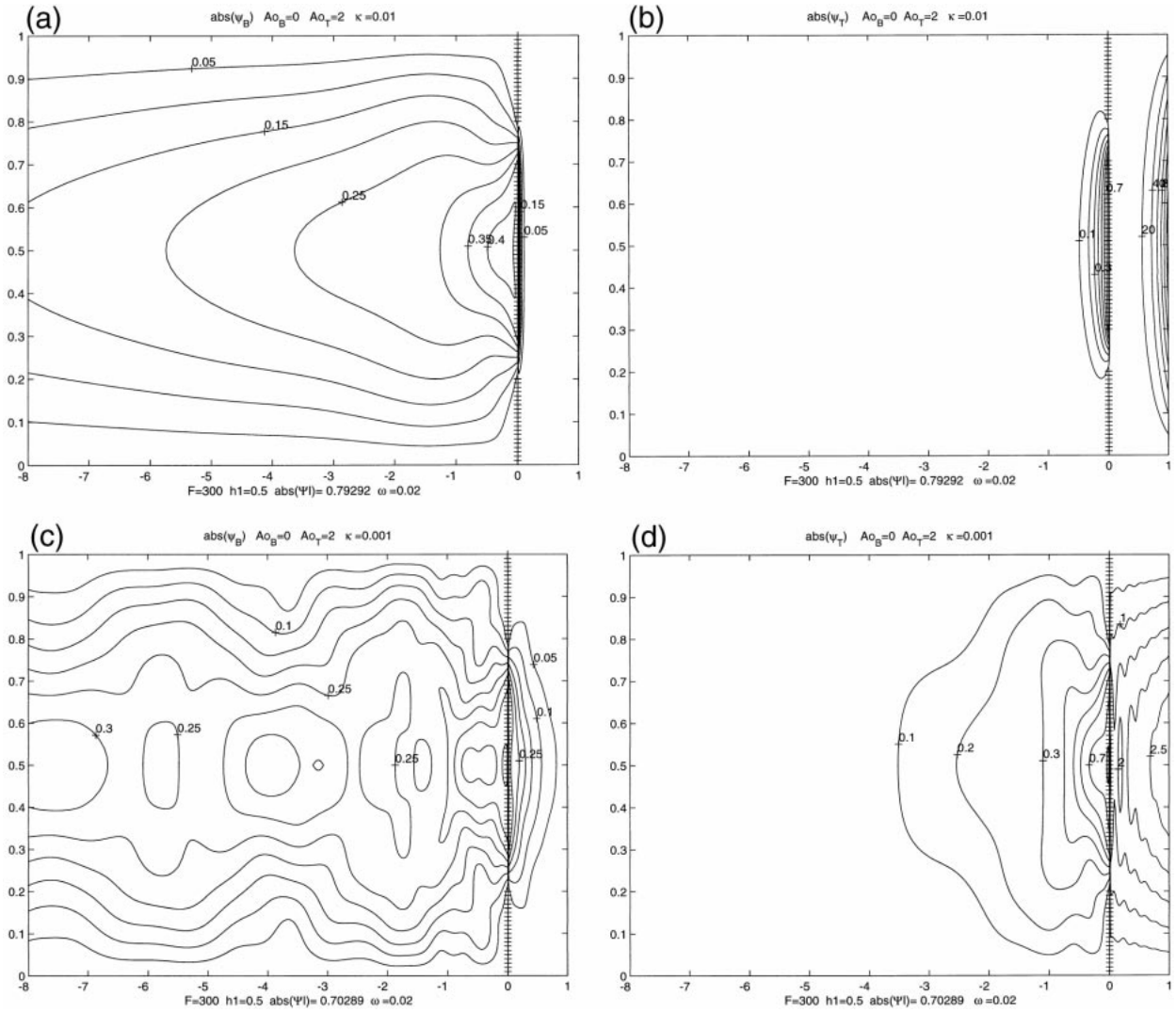

FIG. 4. The same parameters as in Fig. 2 except that $\omega = 0.02$, and $F = 300$, (a) the absolute value of the barotropic wave field; (b) the baroclinic wave field. (c) As in (a) but for $\kappa = 0.001$; (d) as in (b) for $\kappa = 0.001$.

$$\left(\frac{\partial}{\partial t} + \kappa\right) \iint_{A_j} (\psi_2 - \psi_1) F_2 h_2 \, dx \, dy$$

$$= S_{2j} - \iint_{A_j} w_* \, dx \, dy, \tag{2.5}$$

where the integral in (2.5) occurs in each completely enclosed subbasin. Thus in the case pertaining to Fig. 1a there is a single area integral in (2.5) extending over the full domain of the lower layer. In the case of Fig. 1b, that is, of partial gaps, in which the two subbasins in the lower layer are isolated geographically, the constraint (2.5) is applied separately to each subbasin. In (2.5) the first term on the right-hand side represents the net boundary inflow, that is, the inward normal velocity integrated around the closed basin, and is thus a measure of the ageostrophic net source of mass for that basin. The second term on the right-hand side measures the area averaged net passage of fluid between the layers. The difference of the two terms requires a net storage of mass in the lower layer, that is, a nonzero value of the left-hand side of (2.5). That forcing term can be specified arbitrarily and, for simplicity, we will assume here that the left-hand side of (2.5) is zero so that the constraint becomes a homogeneous condition on the net interface displacement. This reserves the forcing in the problem to the potential vorticity sources appearing in (2.1).

Thus in the case of the complete gaps (Fig. 1a) there are three constants to determine (Ψ_{I1}, Ψ_{I2}, Ψ_2), which are determined with the aid of the two circulation conditions of (2.4) applied in each layer and the single mass condition of (2.5). When the gaps are partial (Fig. 1b), the unknown constants are (Ψ_{I1}, Ψ_2^R, Ψ_2^L), and the con-

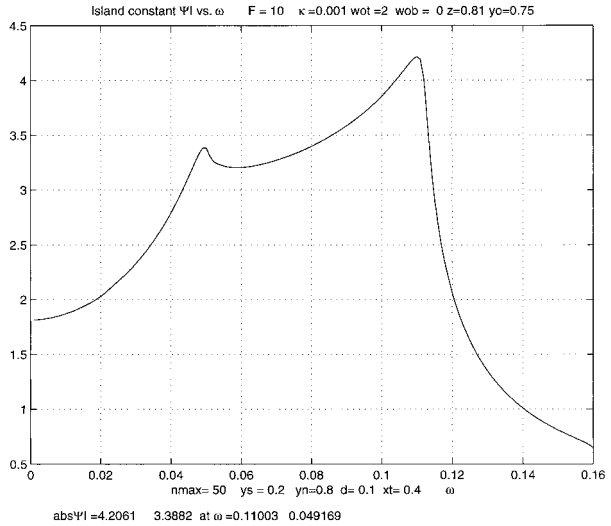

FIG. 5. The response of Ψ_{I1} vs forcing frequency for the case of partial gaps and $F = 10$, $\kappa = 0.001$. The forcing is purely baroclinic.

ditions to be applied are the circulation condition in only the upper layer and the mass conservation condition (2.5) in each of the two isolated subbasins of layer 2.

In the case when the eastern and western boundaries are open so that the eastern and western subbasins are considered infinite in extent, the integral mass constraints become irrelevant and the constants Ψ_2^L, Ψ_2^R can both be set equal to zero. Although this is intuitively obvious, I shall demonstrate this in detail during the discussion of the normal mode problem of section 5.

Although the presence of the partial gap geometry mixes barotropic and baroclinic vertical modes, it is useful to approach the solution of the problem in terms of the barotropic and baroclinic streamfunctions. Thus, defining

$$\psi_B = h_1\psi_1 + h_2\psi_2, \tag{2.6a}$$

$$\psi_T = \psi_1 - \psi_2, \tag{2.6b}$$

the system (2.1) can be rewritten

$$\left(\frac{\partial}{\partial t} + \kappa\right)[\nabla^2\psi_B] + \frac{\partial\psi_B}{\partial x} = w_e \equiv T_B \tag{2.7a}$$

$$\left(\frac{\partial}{\partial t} + \kappa\right)[\nabla^2\psi_T - 2F\psi_T] + \frac{\partial\psi_T}{\partial x} = \frac{w_e}{h_1} - \frac{w_*}{h_1h_2} \equiv T_T, \tag{2.7b}$$

where T_B, T_T are the barotropic and baroclinic source terms for potential vorticity and

$$F = \frac{f_o^2L^2H}{g'H_1H_2}.$$

Note that in terms of the baroclinic and barotropic streamfunctions the layer streamfunctions are

$$\psi_1 = \psi_B + h_2\psi_T, \tag{2.8a}$$

$$\psi_2 = \psi_B - h_1\psi_T. \tag{2.8b}$$

3. Waves incident on the barrier

In this section we consider the interaction of a wave, incident from the east, on a barrier, or ridge, spanning the basin. The domain in the x, or zonal, direction is semi-infinite on either side of the barrier. To start, we consider a barrier that completely blocks the lower layer but is absent entirely from the upper layer. Thus, in this case, there is a free pathway for the wave in the upper layer to traverse the barrier. We consider waves at frequency ω.

The solutions of (2.7a,b) may be written, in the region $x \geq x_t$.

$$\psi_B = e^{i\omega t}\sum_{n=1}^{\infty} A_n \sin(n\pi y)e^{i(k-a_n)(x-x_t)} + e^{i\omega t}\sum_{n=1}^{\infty} B_n \sin(n\pi y)e^{i(k+a_n)(x-x_t)}, \tag{3.1a}$$

$$\psi_T = e^{i\omega t}\sum_{n=1}^{\infty} D_n \sin(n\pi y)e^{i(k-b_n)(x-x_t)} + e^{i\omega t}\sum_{n=1}^{\infty} E_n \sin(n\pi y)e^{i(k+b_n)(x-x_t)}, \tag{3.1b}$$

where

$$k = 1/(2\omega) \tag{3.2a}$$

$$a_n = (k^2 - n^2\pi^2)^{1/2} \tag{3.2b}$$

$$b_n = (k^2 - n^2\pi^2 - F)^{1/2}. \tag{3.2c}$$

In (3.1) the solution consists of an incident wave whose structure in y is represented by the Fourier sine series with coefficients A_n. For a given frequency and Fourier modal number there are two x wavenumbers that are possible. Since the incident wave has its energy directed to the west, it must consist of the long wave, and this accounts for the minus sign in the exponential factor for that wave field. Also for a given frequency, when the y-modal number becomes large enough, the wave must decay in the direction of propagation, which also determines the choice of sign. The reflected barotropic wave has amplitude B_n at for each y mode and has the short x scale associated with the plus sign in the second term in (3.1a). The wavenumber factors a_n and b_n are those appropriate for the barotropic and baroclinic portions of the waves respectively.

Dissipation may be included in the solution be redefining k as

$$k = \frac{1}{2(\omega - i\kappa)} \tag{3.3}$$

in (3.1) and (3.2).

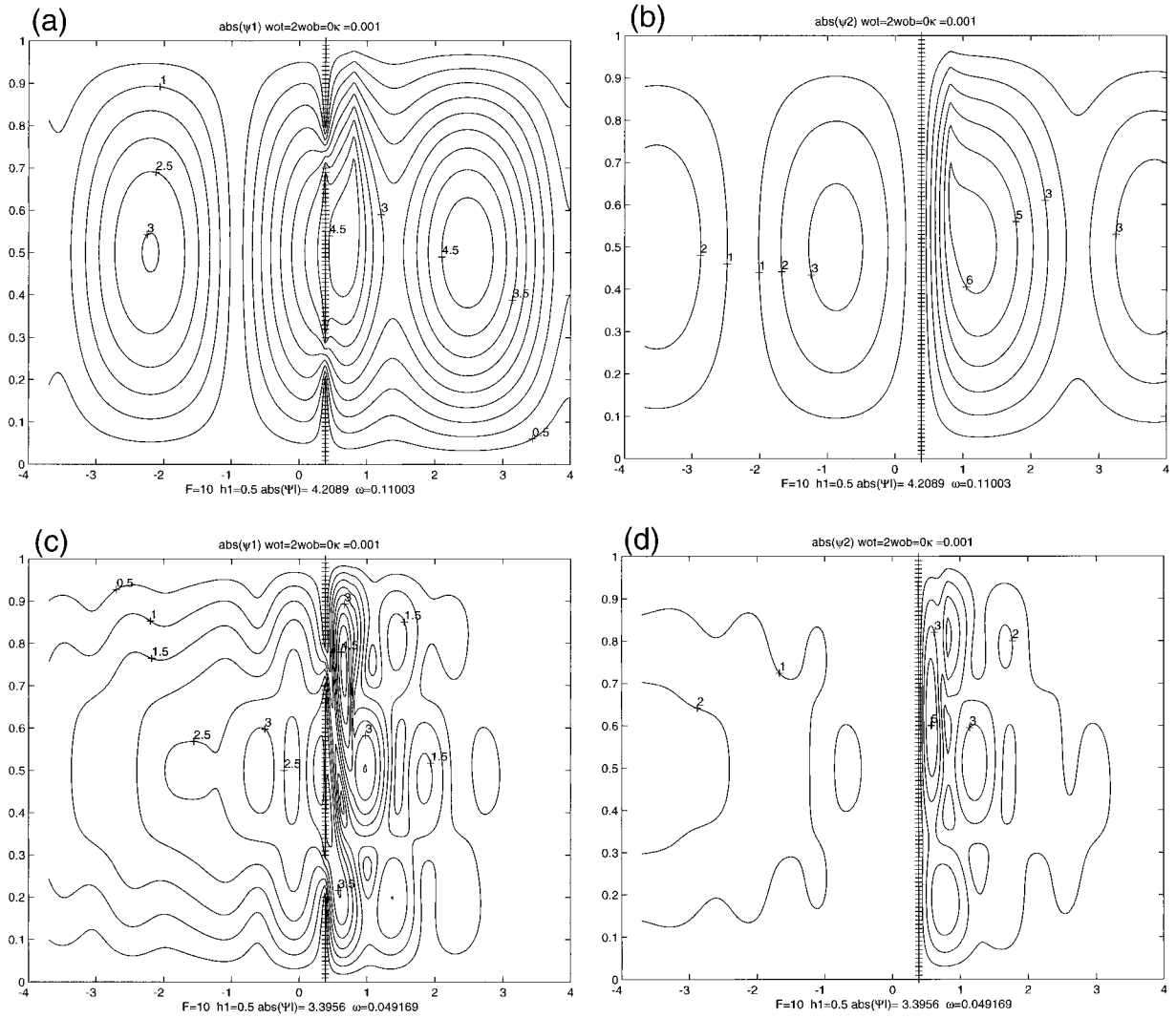

FIG. 6. The modulus of the forced solution in the two layers for the parameters of Fig. 5 for $\omega = 0.110\,03$ (a) the upper-layer streamfunction and (b) the lower-layer amplitude: (c) and (d) as in (a) and (b) but for $\omega = 0.049\,169$.

For $x \leq x_t$ the solution may be written,

$$\psi_B = e^{i\omega t} \sum_{n=1}^{\infty} C_n \sin(n\pi y) e^{i(k-a_n)(x-x_t)}, \qquad (3.4a)$$

$$\psi_T = e^{i\omega t} \sum_{n=1}^{\infty} G_n \sin(n\pi y) e^{i(k-b_n)(x-x_t)}; \qquad (3.4b)$$

that is, in the transmitted wave only the wave with group velocity directed westward appears.

On $x = x_t$ the lower-layer streamfunction must be zero and the upper-layer streamfunction must be continuous and have a continuous first derivative in x. With (2.6), (3.1), and (3.4) this yields the reflected and transmitted wave amplitudes in terms of the incident wave amplitudes; that is,

$$B_n = h_2 b_n \frac{[h_1 D_n - A_n]}{[h_1 a_n + h_2 b_n]} \qquad (3.5a)$$

$$C_n = h_1 \frac{[a_n A_n + b_n h_2 D_n]}{[h_1 a_n + h_2 b_n]} \qquad (3.5b)$$

$$E_n = \frac{[a_n A_n - h_1 a_n D_n]}{[h_1 a_n + h_2 b_n]} \qquad (3.5c)$$

$$G_n = \frac{[a_n A_n + b_n h_2 D_n]}{[h_1 a_n + h_2 b_n]}. \qquad (3.5d)$$

It is important to note that as a consequence of the interaction with the topography there is an order one transformation of the vertical structure of the wave across the barrier. For example, if the incident wave is purely baroclinic, so that $A_n = 0$ for all n, the transmitted

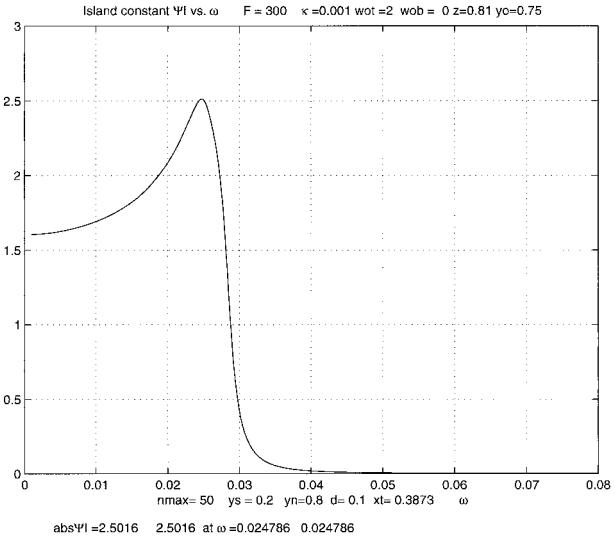

FIG. 7. The response of Ψ_{I1} vs forcing frequency for the case of partial gaps and $F = 300$, $\kappa = 0.001$. The forcing is purely baroclinic. Compare with Fig. 5.

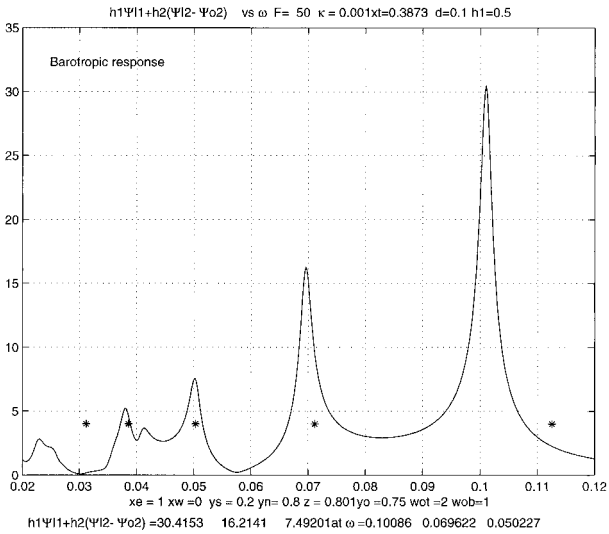

FIG. 9. The response curve for the barotropic mass flux through the gaps as a function of frequency for $\kappa = 0.001$ for the full gap case. The asterisks in the figure mark the barotropic normal mode frequencies for the barrier-free basin.

wave will have a barotropic component given by C_n in (3.5c). The baroclinic incident wave thus has an order one portion of its energy scattered into the barotropic field. In particular, west of the ridge the solution in each layer, in terms of the incident wave amplitudes, is

$$\psi_1 = e^{i\omega t} \sum_{n=1}^{\infty} \sin(n\pi y) \frac{(a_n A_n + h_2 b_n D_n)}{(h_1 a_n + h_2 b_n)} \times \{h_1 e^{i(k-a_n)(x-x_t)} + h_2 e^{i(k-b_n)(x-x_t)}\}, \quad (3.6a)$$

$$\psi_2 = e^{i\omega t} \sum_{n=1}^{\infty} \sin(n\pi y) h_1 \frac{(a_n A_n + h_2 b_n D_n)}{(h_1 a_n + h_2 b_n)} \times \{e^{i(k-a_n)(x-x_t)} - e^{i(k-b_n)(x-x_t)}\}. \quad (3.6b)$$

Note that in the limit of very strong stratification, that is, when the deformation radius is much larger than the basin scale so that $F \to 0$, $a_n \to b_n$ and the streamfunction in the lower layer vanishes. That is, in this limit the bottom topography completely shields the lower layer in the western basin from the impinging energy from the east. On the other hand, as F gets very large, for a given frequency and hence a given k, the baroclinic portion of the field, represented by the second exponential in the solution, decays westward more rapidly than the barotropic portion, leaving the barotropic field dominant and thus exciting motion in the lower layer west of the barrier. This can easily be seen as follows. Consider the frequency in the range where both the

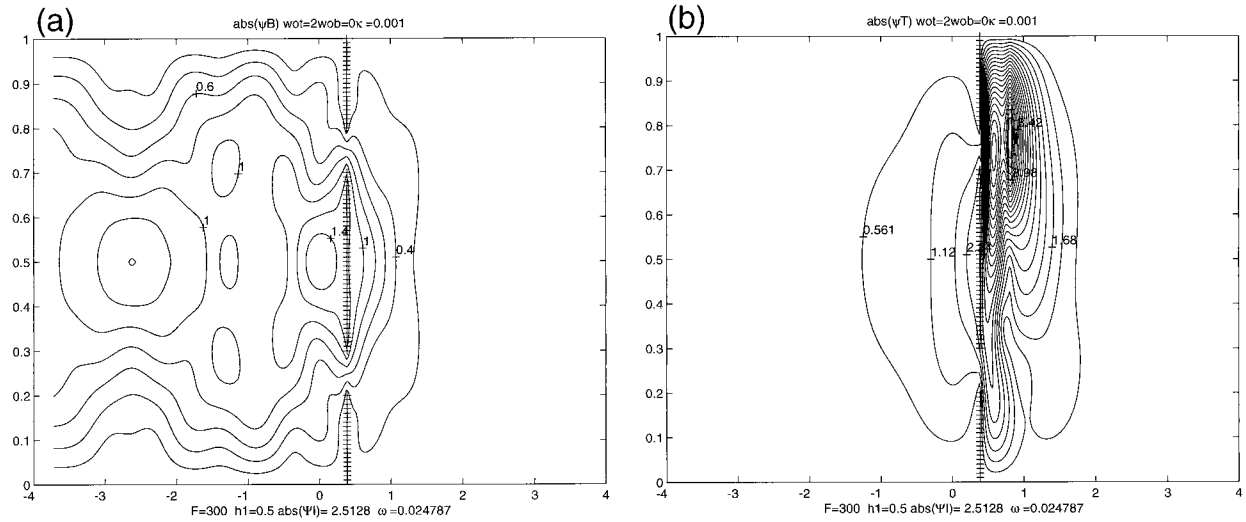

FIG. 8. The modulus of (a) the barotropic and (b) the baroclinic streamfunctions for the parameters of Fig. 7 and for $\omega = 0.024\,787$.

baroclinic and barotropic waves, or at least the low n modes, can be propagating. Further, we suppose there is a slight dissipation so that

$$k = k_r + ik_i = \frac{\omega}{2(\omega^2 + \kappa^2)} + i\frac{\kappa}{2(\omega^2 + \kappa^2)}. \quad (3.7)$$

This yields a complex x wavenumber for the barotropic and baroclinic portions of the solution. If κ is small compared to ω, then the imaginary part of the wavenumber, which yields the spatial decay scale westward, is for both the barotropic and baroclinic parts of the field

$$\mathrm{Im}(k - a_n) = k_i\left(\frac{k_r}{\sqrt{k_r^2 - n^2\pi^2}} - 1\right), \quad (3.8a)$$

$$\mathrm{Im}(k - b_n) = k_i\left(\frac{k_r}{\sqrt{k_r^2 - n^2\pi^2 - F}} - 1\right). \quad (3.8b)$$

If the frequency is in the range that allows baroclinic wave propagation, both radicals in (3.8) will be real (and positive) but the radical involving F will be smaller, leading to a larger spatial decay rate for the baroclinic field. For large enough n, so that both a_n and b_n are imaginary, the baroclinic component will again decay more rapidly. There is thus a general tendency for the barotropic part of the field to dominate the solution west of the ridge, even if the incident wave field is purely baroclinic. As we shall see, this general tendency is common to all the cases to be described below even when, and sometimes especially when, the upper layer is also partially blocked.

When there is a barrier in the upper layer as well as the lower layer, the forms of the solutions (3.1) and (3.4) still are valid but the matching conditions at the longitude of the ridge change. Consider the streamfunction in the upper layer. As in PS we assume that for narrow enough gaps, that is for $d \ll 1$, the streamfunction at the longitude of the barrier and gaps can be approximated as

$$\psi_n = \Psi_n e^{i\omega t}\begin{cases} 0, & 0 \le y \le y_s \\ (y - y_s)/d, & y_s \le y \le y_s + d \\ 1, & y_s + d \le y \le y_n - d \\ (y_n - d)/d, & y_n - d \le y \le y_n \\ 0, & y_n \le y \le 1 \end{cases} \quad (3.9)$$

for each layer for which gaps occur between y_s and $y_s + d$ and $y_n - d$ and y_n.

Pedlosky and Spall showed that this representation of the streamfunction at that longitude is adequate as long as the scale of the wave is large compared to the gap width and that is precisely the situation of current interest. This assumes that within each gap the flow is unidirectional at each moment.

This broken line profile for ψ is represented by the Fourier sine series,

$$\psi_n = \Psi_n e^{i\omega t}\sum_{n=1}^{\infty} g_{n2}\sin(n\pi y) \quad (3.10)$$

where

$$g_{n2} = \left(\frac{2}{dn^2\pi^2}\right)[\sin(n\pi[y_s + d]) - \sin(n\pi y_s) - \sin(n\pi y_n) + \sin(n\pi[y_n - d])], \quad (3.11)$$

whose form as a function of n is shown in Fig. 2. Clearly, it is the lowest meridional modes that are favored for transmission. Note that for the case where the gaps are placed symmetrically with respect to the midlatitude of the basin, g_{n2} vanishes for even n.

Consider, first the case in which the gaps occur only in the upper layer. Then, at $x = x_t$ the lower-layer streamfunction must be zero so that the matching conditions become

$$A_n + B_n + h_2(D_n + E_n) = \Psi_{I1}h_1 g_{n2} = C_n + h_2 G_n \quad (3.12a)$$

$$A_n + B_n - h_1(D_n + E_n) = \quad 0 \quad = C_n - h_1 G_n. \quad (3.12b)$$

The final condition to be applied is the circulation condition that here requires the integral of the meridional velocity along the length of the island segment to be equal on each side of the barrier. This condition, with (3.12), determines the island constant Ψ_{I1} in terms of the amplitude of the incident wave as

$$\Psi_{I1} = \frac{\sum g_{n3}\{a_n A_n + h_2 b_n D_n\}}{\sum g_{n3}g_{n2}\{h_1 a_n + h_2 b_n\}}, \quad (3.13)$$

where the sums in (3.13) run over all n and where

$$g_{n3} = (\cos n\pi[y_s + d] - \cos n\pi[y_n - d])/n\pi. \quad (3.14)$$

Once Ψ_{I1} is known, each of the transmitted and reflected wave amplitudes can be determined from (3.12). In particular, for the transmitted wave field,

$$\psi_1 = e^{i\omega t}\Psi_{I1}\sum_n g_{n2}\sin n\pi y\{h_1 e^{i(k-a_n)(x-x_t)} + h_2 e^{i(k-b_n)(x-x_t)}\} \quad (3.15a)$$

$$\psi_2 = e^{i\omega t}\Psi_{I1}\sum_n g_{n2}h_1\sin n\pi y\{e^{i(k-a_n)(x-x_t)} - e^{i(k-b_n)(x-x_t)}\}. \quad (3.15b)$$

The strong similarity between (3.15) and the form of the transmitted wave in the case of the barrier present only in the lower layer (3.6a,b) emphasizes the relative transparency of the upper-layer barrier when there are two gaps. Kelvin's theorem enforces an oscillating meridional velocity on the western side of the barrier in response to the incident wave. The islandlike segment of the barrier then acts as an antenna reradiating energy westward. Note that the transmitted wave amplitude is $O(1)$ even though the gap width is small (and is independent of the gap width in this limit).

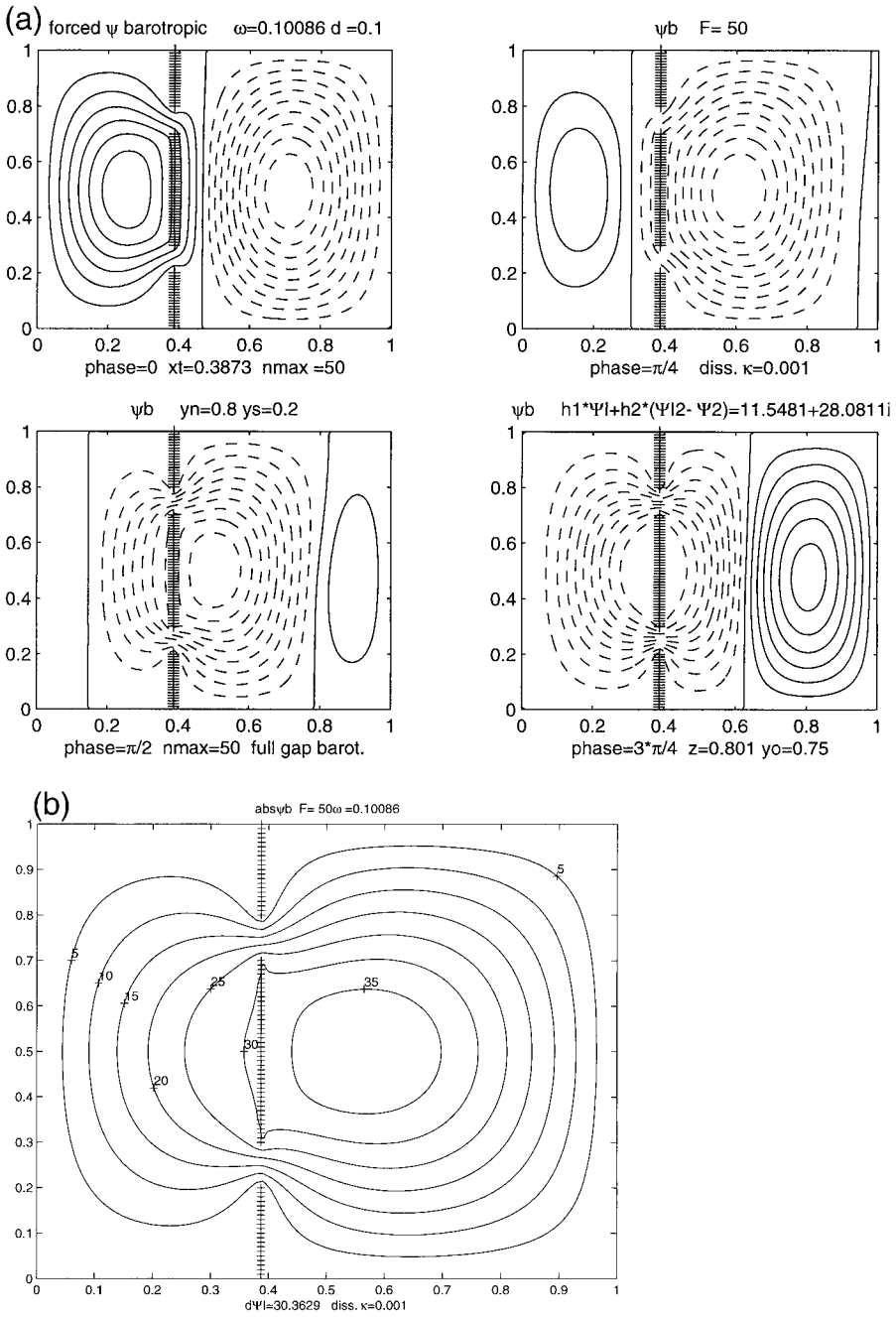

FIG. 10. (a) The barotropic normal mode in the full gap case corresponding to the parameters of Fig. 9 and a frequency $\omega = 0.1008$. (b) Contours of the ''membrane'' function corresponding to the oscillation in (a).

Figure 3 shows the transmission of an incident wave that is purely baroclinic, that is, for which A_n is identically zero. The dissipation parameter $\kappa = 0.01$, while the frequency is low enough (0.03) to lie within the range of propagating baroclinic waves for low meridional wavenumber. Figure 3a shows four snapshots of the wave field in the upper layer as it traverses the barrier slipping through the gaps and radiating westward. Figure 3b shows the *form* of the wave at those same instants in the lower layer. In Figs. 3c and 3d the absolute value of the streamfunction (or the root mean square wave amplitude) in the upper and lower layers is contoured and the contours are labeled, showing clearly the limitation of the transmitted wave to the upper layer for

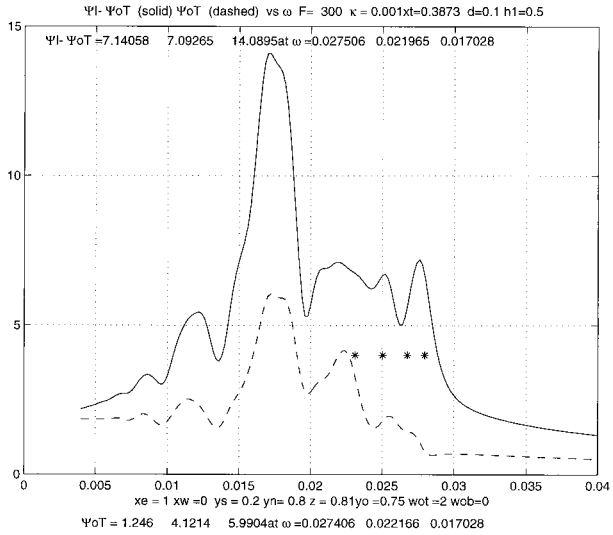

FIG. 11. The response curve for the baroclinic mode for $F = 300$, $\kappa = 0.001$. The solid line is for $\Psi_{IT} - \Psi_T$ as a function of frequency of the forcing, while the dashed line shows Ψ_T as a function of the forcing frequency.

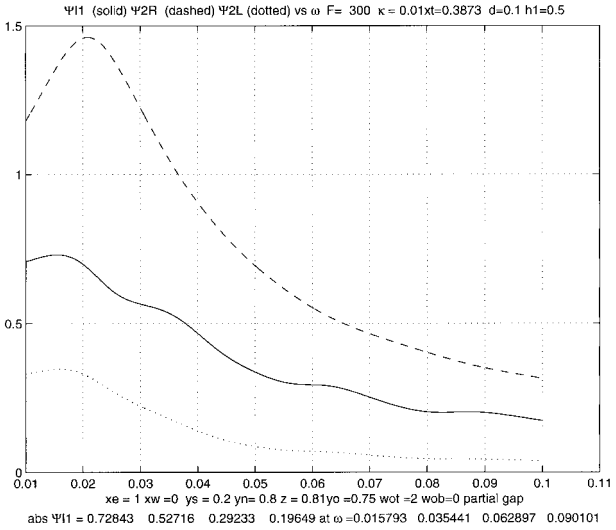

FIG. 13. The response curves for Ψ_{I1}, Ψ_2^R, Ψ_2^L as a function of ω: $F = 300$, $\kappa = 0.01$.

this strongly stratified case. The complete barrier in the lower layer is effective in blocking the transmission of wave energy in the lower layer.

Figure 4 shows the same incident wave (at a slightly lower frequency to allow baroclinic wave propagation) for the case $F = 300$. In this case the deformation radius is small compared to the basin's meridional scale. Figure 4a shows the contours of the absolute value of the barotropic wave field, while Fig. 4b shows the contours of the baroclinic part of the field. Note that the barotropic field east of the ridge is limited to a narrow zone near the ridge. Since the incident wave is purely baroclinic, the barotropic part of the wave field east of the ridge is formed only by the reflected wave field and has short zonal scales. West of the ridge the barotropic wave field reaches rather far to the west in comparison to the baroclinic field, shown in Fig. 3b, which is limited to a zone near the barrier in conformance to the discussion following Eq. (3.8). For smaller values of dissipation ($\kappa = 0.001$) both barotropic and baroclinic wave fields decay more slowly westward but, again, the barotropic field dominates the western region as shown in Figs. 4c and 4d. In this case the ridge is a source of westward propagating barotropic Rossby waves produced by the impinging baroclinic wave.

As in PS, the ability of the incident wave to propagate

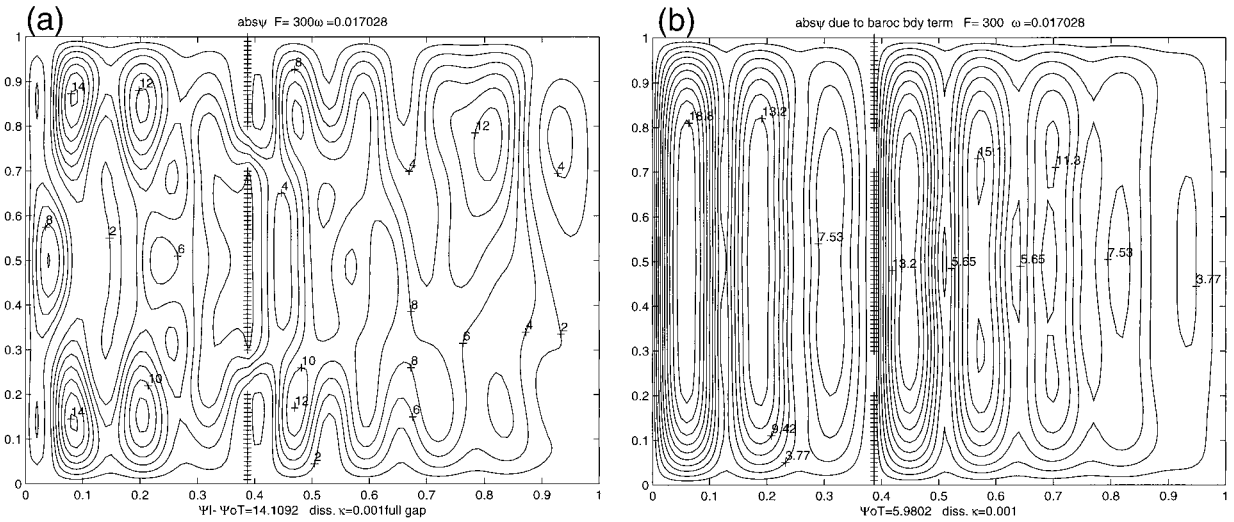

FIG. 12. (a) The mode shape of the absolute value of the baroclinic streamfunction for the parameters of Fig. 11 for $\omega = 0.017\,028$. The asterisks show the first four free normal modes in the absence of the barrier. (b) At the same frequency, the part of the solution corresponding to only the eastern boundary term, i.e., the part proportional to Ψ_T.

through the barrier depends on its meridional structure. In the cases shown the incident wave field is dominated by the $n = 1$ Fourier mode. Examining the parameter g_{n2} defined by (3.11) it follows, as noted earlier, that for gaps placed symmetrically with regard to the center latitude of the basin, g_{n2} is zero for even values of n. Thus, if the incident wave field were composed of only even Fourier modes, that is, if the incident wave field were *antisymmetric* about the midlatitude, there would be no transmission of energy as the Kelvin integral constraint would be automatically satisfied by the meridional velocity on the eastern side of the barrier.

In the case where the gaps extend over both layers, the barotropic and baroclinic modes can be considered separately; that is, the barotropic and baroclinic modes are not mixed by the transfer through the barrier.

The amplitude of the barotropic and baroclinic transmitted waves are then given by

$$C_n = g_{n2}[h_1\Psi_{I1} + h_2\Psi_{I2}] = g_{n2}\left(\frac{\sum_m g_{m3}a_mA_m}{\sum_m g_{m3}g_{m2}a_m}\right) \quad (3.16a)$$

$$G_n = g_{n2}[\Psi_1 - \Psi_2] = g_{n2}\left(\frac{\sum_m g_{m3}b_mD_m}{\sum_m g_{m3}g_{m2}b_m}\right) \quad (3.16b)$$

so that the vertical structure of the wave field is unaltered by the passage through the barrier. A purely baroclinic incident wave will excite only a baroclinic reflected wave and a baroclinic transmitted wave and the wave amplitude in each layer will then be a function only of the vertical structure of the incident wave field. However, if both are present, it will still be true for the reasons outlined in the discussion following (3.8) that the baroclinic wave field will damp more rapidly to the west than will the barotropic part of the field.

4. Forced motion

In this section the problem of the propagation of forced Rossby waves is considered. We imagine a localized source of potential vorticity, oscillating at frequency ω at the position $x = z$, $y = y_o$ located in the eastern subbasin and ask about the response of the fluid, especially in the region west of the barrier, again located at $x = x_t$.

If the forcing in (2.7a,b) is represented as

$$T_B = e^{i\omega t}w_B = e^{i\omega t}\delta(x - z)\sum_n w_{Bn}\sin n\pi y, \quad (4.1a)$$

$$T_T = e^{i\omega t}w_T = e^{i\omega t}\delta(x - z)\sum_n w_{Tn}\sin n\pi y, \quad (4.1b)$$

the equations for the barotropic and baroclinic streamfunctions can be put into canonical form with the transformation

$$(\psi_B, \psi_T) = e^{i\omega t}e^{ik(x-x_t)}[\phi_B, \phi_T], \quad (4.2)$$

where k is defined as in (3.3). The resulting equations for ϕ_B and ϕ_T are

$$\nabla^2\phi_B + k^2\phi_B = -2ikw_Be^{-ik(x-x_t)} \quad (4.3a)$$

$$\nabla^2\phi_T + (k^2 - F)\phi_T = -2ikw_Te^{-ik(x-x_t)}. \quad (4.3b)$$

With the representation of (4.1) the resulting Eqs. (4.3a,b) can be easily solved. The delta function behavior of the pv forcing in x leads to a Green function representation of the solution. In the region east of the forcing a radiation condition is imposed so that only waves with group velocities to the east are retained. West of the barrier only waves with westward group velocity are kept in the solution while in the region between the forcing and the barrier all waves are used and at the barrier the streamfunction in each layer must match the conditions of (3.9) if gaps are present, or else in a layer with no gaps the streamfunction must vanish. We consider in detail the more interesting case of the partial gap solution in which gaps are present only in the upper layer. The streamfunction in the lower layer must vanish, then, at the longitude of the barrier.

It can then be shown that the complete solution is as follows.

In $x > x_t$, the barotropic wave field and baroclinic fields are

$$\psi_B = e^{i\omega t}\sum_n \sin n\pi y\left[h_1\Psi_{I1}g_{n2}e^{i(k+a_n)(x-x_t)} + \frac{kw_{Bn}}{a_n}e^{i(k+a_n)(x-x_t)}e^{-i(k-a_n)(z-x_t)} - \frac{kw_{Bn}}{a_n}\{e^{i(k+a_n)(x-z)}\Theta(x - z) + e^{i(k-a_n)(x-z)}\Theta(z - x)\}\right] \quad (4.4a)$$

$$\psi_T = e^{i\omega t}\sum_n \sin n\pi y\left[\Psi_{I1}g_{n2}e^{i(k+b_n)(x-x_t)} + \frac{kw_{Tn}}{b_n}e^{i(k+b_n)(x-x_t)}e^{-i(k-b_n)(z-x_t)} - \frac{kw_{Tn}}{b_n}\{e^{i(k+b_n)(x-z)}\Theta(x - z) + e^{i(k-b_n)(x-z)}\Theta(z - x)\}\right], \quad (4.4b)$$

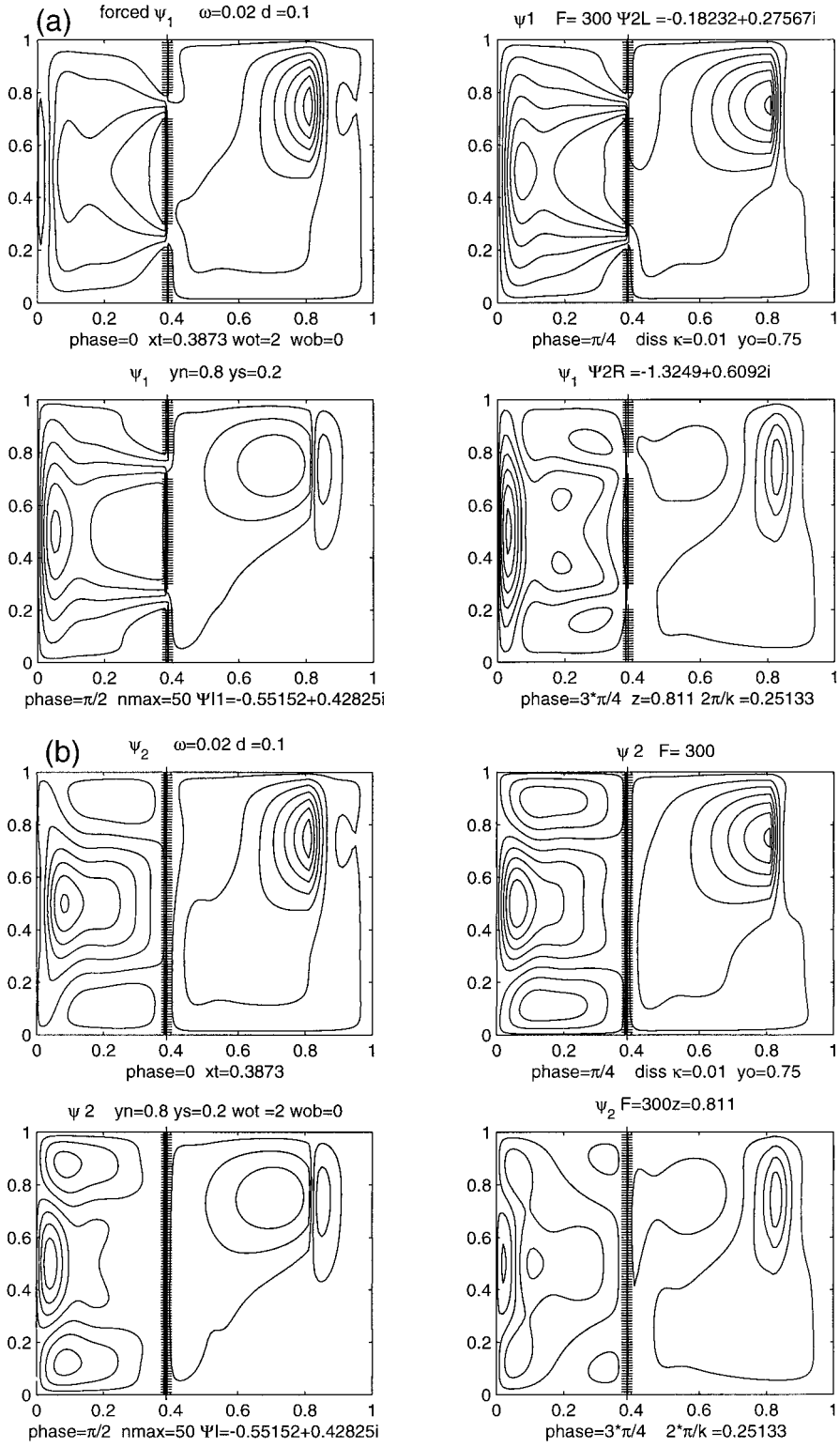

FIG. 14. The wave response for the parameter of Fig. 13 for $\omega = 0.02$ (a) upper layer at four points in the wave period, (b) the lower-layer streamfunction at the same four times, (c) the absolute value of the barotropic streamfunction, and (d) the same for the baroclinic streamfunction.

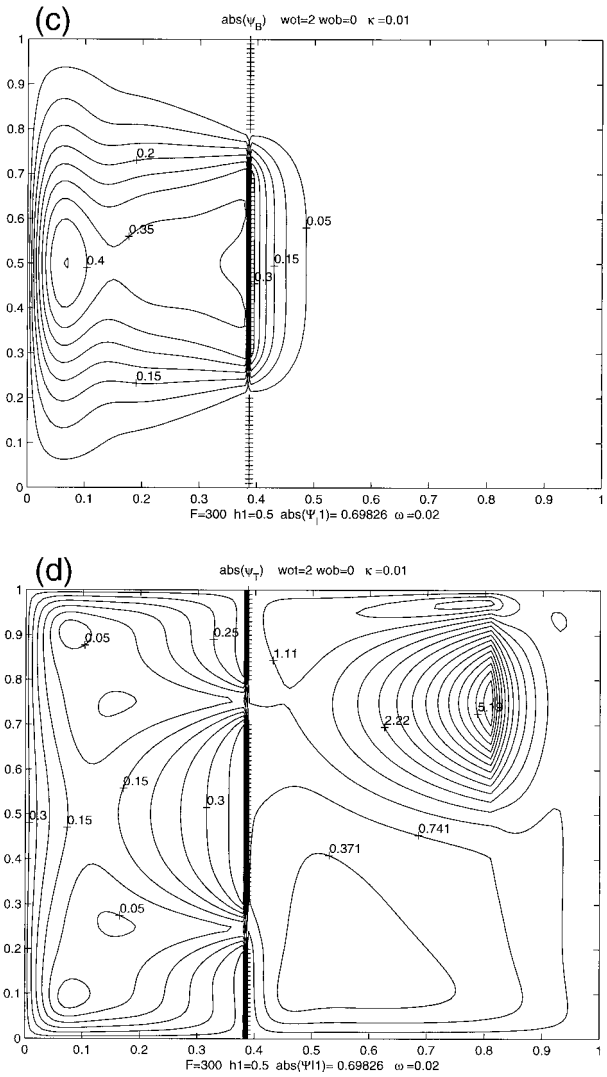

FIG. 14. (*Continued*)

where $\Theta(x)$ is the Heaviside step function, equal to one for positive values of its argument and zero for negative values of its argument.

West of the barrier the solutions are

$$\psi_B = \Psi_{I1} e^{i\omega t} \sum_n h_1 g_{n2} e^{i(k-a_n)(x-x_t)} \sin n\pi y, \quad (4.4c)$$

$$\psi_T = \Psi_{I1} e^{i\omega t} \sum_n g_{n2} e^{i(k-b_n)(x-x_t)} \sin n\pi y \quad (4.4d)$$

so that the solutions for the streamfunction in each layer are given by (3.15a,b). Now, however the island constant, as determined by the circulation condition, is given by

$$\Psi_{I1} = -\frac{k \sum g_{n3}[w_{Bn} e^{-i(k-a_n)(z-x_t)} + w_{Tn} h_2 e^{-i(k-b_n)(z-x_t)}]}{\sum g_{n2} g_{n3}[h_1 a_n + h_2 b_n]}, \quad (4.5)$$

which is analogous to the result (3.13) for free waves impinging on the barrier. It is clear from (4.5) that both barotropic and baroclinic forcing will excite reradiation from the island segment of the barrier, and from (4.4) or (3.15) it follows that there will be a transformation of the nature of the radiated wave across the barrier.

Figure 5 shows the response curve for Ψ_{I1} as a function of forcing frequency for the case where the forcing, that is, the pv source, is purely baroclinic: ($w_{bn} = 0$) and $F = 10$. Naturally, the motion in the western basin will be more efficiently forced where this response curve has its peaks. In this case the interface between the two layers is fairly rigid since F is rather small: the dissipation, $\kappa = 0.001$. We note there are two broad peaks to the response. It is interesting to note that in the absence of the barrier the highest frequency for a baroclinic free Rossby wave for a given meridional mode is given by

$$\omega_{T\max} = \frac{1}{2(n^2\pi^2 + F)^{1/2}}. \quad (4.6)$$

For $n = 1$ this corresponds to a frequency 0.112 very close to the first peak in Fig. 5, which occurs at 0.110 03. For the *third* meridional mode, $n = 3$, the maximum frequency for (4.6) would be 0.0503, very close to the second peak in Fig. 5, which occurs at 0.049 17. A peak for $n = 2$ would not be expected since, as explained above, motions antisymmetric about the midlatitude yield no transmitted motion since the circulation theorem is satisfied for a wave limited to the eastern basin. Figure 6 shows the absolute value of the streamfunction in the upper and lower layers for forcing at $\omega = 0.110\,03$. The motion is strongly baroclinic with a displacement in x of the maxima of the amplitudes of the transmitted motions. Note that the meridional motion is dominated by the $n = 1$ Fourier mode. A similar figure (Fig. 6c) for the mode at $\omega = 0.049\,17$ shows a dominance of the $n = 3$ mode.

For larger values of F the differences between the baroclinic and barotropic waves become even more pronounced, and the transformational character of the interaction with topography becomes, once again, more dramatic.

Figure 7 shows the response curve for the island constant as a function of frequency for $F = 300$ and for κ, once again, $= 0.001$. The roll-off of the response curve occurs at a frequency slightly smaller than 0.03 and it is interesting to note from (4.6) that this occurs very near the maximum baroclinic wave frequency for these parameters (0.0284).

In this case it is more illuminating to examine the baroclinic and barotropic components of the wave field. These are seen in Fig. 8. In Fig. 8a we see the barotropic portion of the wave field. Since the forcing is purely baroclinic (as we might expect from a eddy forcing of PV due to localized baroclinic instability in the eastern basin), the barotropic field is produced by the topography, which is seen to act as a source of barotropic

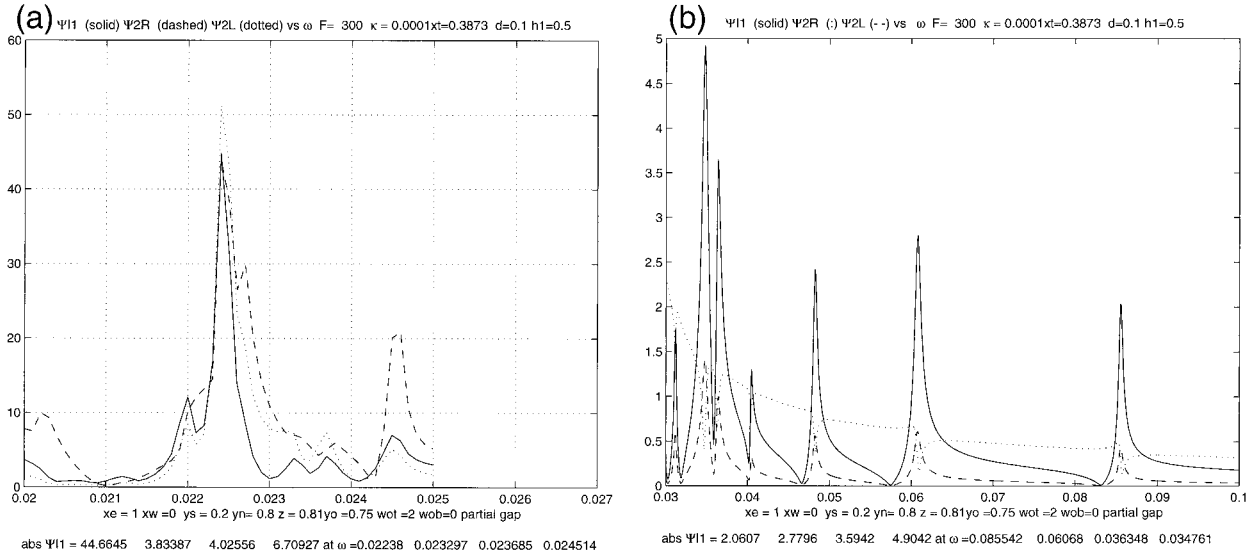

FIG. 15. The response curve for Ψ_{I1}, Ψ_2^R, Ψ_2^L as a function of ω for $F = 300$ and $\kappa = 0.001$: (a) the frequency range from 0.02 to 0.03, and (b) the interval from 0.03 to 0.1.

wave energy. There is a small amount of such radiation eastward from the island segment consisting of short zonal waves. Most of the radiation is westward at longer wavelengths. Figure 8b shows the baroclinic portion of the field. It is very large near the forcing region at $x = 0.81$, $y = 0.75$. It decays rapidly west of the barrier so that the transmitted wave is dominated by the barotropic part of the field, in a manner similar to the transmission and transformation of wave energy of free waves described in section 3. For the sake of brevity, only the solutions corresponding to purely baroclinic forcing have been shown but similar results occur for other forcings; that is, the barotropic mode dominates in the transmitted radiation for the reasons described in the discussion following Eqs. (3.8).

If the gaps are present in each layer, the response of the fluid to the barotropic and baroclinic forcing are decoupled and can be dealt with separately. The transmission properties still depend on the meridional structure of the forcing: for example, Kelvin's theorem still governs the transmission; however, there is no transformation of wave type and so it will not be discussed in any further detail.

5. Closed basins

When the basin's meridional boundaries are taken into account so that reflections from the western and eastern boundaries of the basin can be considered explicitly, it is necessary to add to the machinery of solution the constraints of mass conservation discussed in section 2. It is then necessary to explicitly allow the streamfunction to be nonzero on the basin boundaries and the constants (Ψ_{I1}, Ψ_2^R, Ψ_2^L) in the case of the partial barrier, or the constants (Ψ_{I1}, Ψ_{I2}, Ψ_2) for full depth gaps, must all be found as part of the solution. In the following impermeable meridional boundaries are placed at $x = x_w$ on the west and at $x = x_e$ on the eastern edge of the basin with the barrier at an intermediate position x_t.

Since the solution is no longer zero on the boundaries at $y = 0$ and $y = 1$, the form of the solution must be altered. The Fourier sine series could still be used to represent the solution but it would converge very slowly. It is useful instead to look for solutions to (2.7a,b) in the form

$$\psi_B = e^{i\omega t}\Psi_B^{R,L} + e^{i(\omega t + k(x - x_t))}\phi_B(x, y), \qquad (5.1a)$$

$$\psi_T = e^{i\omega t}\Psi_T^{R,L}\frac{\cosh\lambda(y - 1/2)}{\cosh(\lambda/2)} + e^{i(\omega t + k(x - x_t))}\phi_T(x, y), \qquad (5.1b)$$

where $\lambda = F^{1/2}$ and Ψ_B and Ψ_T are constants whose superscripts L, R refer to the regions to the right and left, respectively, where they are pertinent. These constants are chosen satisfy the inhomogeneous boundary conditions on $y = 0$ and $y = 1$. In the case where the gaps extend into the lower layer these constants must be the same on the left and right-hand sides of the barrier, while in the case of partial gaps, they differ. The functions ϕ_B and ϕ_T satisfy (4.3a,b). These functions now satisfy homogeneous boundary conditions on $y = 0, 1$ and may be expanded in a rapidly converging Fourier sine series.

Again, the forcing functions will be taken to be localized in the eastern subbasin with delta function structure in x and an approximate delta function structure in y (to allow a more rapid convergence of the Fourier sine representation the forcing is smeared a small amount in y). The details of the solutions of the resulting differential equations are lengthy but straightforward and the

details are not presented here for the sake of brevity. We outline here only the steps required to reach the final solution. It is somewhat clearer to consider the two cases of the full gap and partial gap geometries separately.

a. Full gaps

In the case of full gaps the boundary constants are the same in the eastern and western subbasins. Physically, this is because the Kelvin waves, not explicitly present in quasigeostrophic theory but responsible for setting the boundary constants, can pass from one subbasin to the next through the gaps joining the boundaries together. The superscripts R and L for the constants are therefore not required. If we again arbitrarily take $\Psi_1 = 0$, the barotropic and baroclinic boundary constants are related to Ψ_2; that is,

$$\Psi_B = h_2\Psi_2, \tag{5.2a}$$

$$\Psi_T = -\Psi_2. \tag{5.2b}$$

Since the gaps are complete, the baroclinic and barotropic responses to the forcing are independent of one another and can be considered separately. The barotropic response is, for $x > x_t$,

$$\psi_B = \Psi_B e^{i\omega t} + e^{i(\omega t + k(x-x_t))}\Delta\Psi_I \sum_n \sin n\pi y g_{n2}\frac{\sin a_n(x-x_e)}{\sin a_n(x_t-x_e)} + e^{i(\omega t + k(x-z))}\sum_n \sin n\pi y\left(\frac{2kw_{Bn}}{ia_n}\right)$$
$$\times\left[\Theta(x-z)\frac{\sin a_n(x_t-z)\sin a_n(x-x_e)}{\sin a_n(x_t-x_e)} + \Theta(z-x)\frac{\sin a_n(z-x_e)\sin a_n(x_t-x)}{\sin a_n(x_t-x_e)}\right], \tag{5.3a}$$

while for $x < x_t$, the barotropic solution is given by

$$\psi_B = \Psi_B e^{i\omega t} + e^{ik(x-x_t)}\Delta\Psi_I \sum_n g_{n2}\sin n\pi y\frac{\sin a_n(x-x_w)}{\sin a_n(x_t-x_w)}, \tag{5.3b}$$

where we define

$$\Delta\Psi_I \equiv h_1\Psi_{I1} + h_2(\Psi_{I2} - \Psi_2) \tag{5.4}$$

and, thus, the amplitude of the barotropic flux through two gaps. Note that the barotropic solution depends only on this constant, in addition to the forcing, and is independent of the boundary constants associated with the interface displacement, which enter only in the solution of the baroclinic mode. The flux constant in (5.4) can be determined, in the full gap case by the *barotropic* component of the Kelvin constraint, that is, by the application of (2.4) to the barotropic component of the meridional velocity on each side of the ridge segment. This yields

$$\Delta\Psi_I = \frac{-e^{-ik(z-x_t)}\sum 2ikw_{Bn}g_{n3}\dfrac{\sin a_n(z-x_e)}{\sin a_n(x_t-x_e)}}{\sum a_n g_{n3}g_{n2}\dfrac{\sin a_n(x_e-x_w)}{\sin a_n(x_t-x_e)\sin a_n(x_t-x_w)}}. \tag{5.5}$$

The vanishing of the denominator in (5.5) occurs at the natural frequencies of oscillation for the barotropic mode in the basin and agrees with the normal mode dispersion relation in PS. We consider here the case when κ is not zero so that the free normal modes will be damped. The forced solution, for small κ, will be resonant at those natural frequencies of oscillation (corresponding to the full basin modes that involve flow through the barrier's gaps). In fact, examining the resonant frequencies for small but nonzero κ is a convenient way to find the natural modes of oscillation.

Before discussing the nature of the barotropic solution, it is of interest to consider the baroclinic mode in this full gap case.

The baroclinic solution is, for $x > x_t$,

$$\psi_T = \Psi_T e^{i\omega t}\frac{\cosh\lambda(y-1/2)}{\cosh\lambda/2} + e^{i\omega t}\sum_n \sin n\pi y\left\{\Psi_T g_{n1}\left[\frac{\sin b_n(x-x_e)}{\sin b_n(x_t-x_e)}e^{ik(x-x_t)} + \frac{\sin b_n(x_t-x)}{\sin b_n(x_t-x_e)}e^{ik(x-x_e)}\right]\right.$$
$$+ (\Psi_{IT} - \Psi_T)g_{n2}\frac{\sin b_n(x-x_e)}{\sin b_n(x_t-x_e)}e^{ik(x-x_t)}$$
$$- \frac{2ikw_{Tn}}{b_n}e^{ik(x-z)}\left[\Theta(x-z)\frac{\sin b_n(x-x_e)\sin b_n(x_t-z)}{\sin b_n(x_t-x_e)}\right.$$
$$\left.\left. + \Theta(z-x)\frac{\sin b_n(z-x_e)\sin b_n(x_t-x)}{\sin b_n(x_t-x_e)}\right]\right\}, \tag{5.6a}$$

while for $x < x_t$,

$$\psi_T = e^{i\omega t}\Psi_T \frac{\cosh\lambda(y - 1/2)}{\cosh\lambda/2} + e^{i\omega t}\sum_n \sin n\pi y\left[\Psi_T g_{n1}\left(\frac{\sin b_n(x - x_w)}{\sin b_n(x_t - x_w)}e^{ik(x-x_t)} + \frac{\sin b_n(x_t - x)}{\sin b_n(x_t - x_w)}e^{ik(x-x_w)}\right)\right.$$
$$\left. + (\Psi_{IT} - \Psi_T)g_{n2}\frac{\sin b_n(x - x_w)}{\sin b_n(x_t - x_w)}e^{ik(x-x_t)}\right], \quad (5.6b)$$

where

$$\Psi_{IT} \equiv \Psi_{I1} - \Psi_{I2}, \quad (5.7a)$$

$$g_{n1} = \frac{2(1 - (-1)^n)F}{n\pi(F + n^2\pi^2)}. \quad (5.7b)$$

The baroclinic mode presents some new features of interest. It is, of course, independent of the barotropic mode and the barotropic forcing in the full gap case. But it is especially clear from (5.7b) that the radiation beyond the barrier is more complex than in the barotropic mode case or in the case of the baroclinic motion in the absence of closed meridional boundaries. The new term in the solution, proportional to $\Psi_T g_{n1}$ reflects the passage of the Kelvin wave around the entire boundary of the basin (an impossibility in the open boundary limit), which sets up an oscillation of the interface on both the eastern boundary of the complete basin and the eastern boundary of the western subbasin. This *y*-independent disturbance of the interface to the east of each of the subbasins forces a westward propagating Rossby wave. A similar phenomenon is present in the work of Kawase (1987), and a similar phenomena also occurs in the linear steady state model of Edwards and Pedlosky (1995). We note, in examining the form of (5.7b) that this portion of the solution does not depend on the presence of the two gaps and, in fact, would be present were there only a single gap (hence the subscript 1 for the function g_{n1}). Thus for the *baroclinic* mode there is an additional mechanism to provide the reradiation of the wave through the barrier in addition to the antenna mechanism springing from Kelvin's theorem.[1]

In order to determine the two constants required for the complete solution, Ψ_T and Ψ_{IT}, it is necessary to apply the baroclinic component of the Kelvin circulation constraint, that is, the circulation of the vertical shear of the meridional velocity and the condition of mass conservation (2.5) applied to the entire basin. Using the solution for ψ_T given above these two constraints yield two algebraic equations for Ψ_T and Ψ_{IT}. Assuming that there is no mass storage in the basin, so that the right-hand side of (2.5) is zero, the two constraints lead to equations of the form

$$C_1\Psi_T + C_2(\Psi_{IT} - \Psi_T) = X_1, \quad (5.8a)$$

$$C_3\Psi_T + C_4(\Psi_{IT} - \Psi_T) = X_2. \quad (5.8b)$$

The coefficients in (5.8) are given in appendix A. The solution of (5.8) completes the solution of the baroclinic, forced problem in a bounded basin. Before describing the nature of the solutions for both the barotropic and baroclinic problems in the full gap case, it is important to note, from Eqs. (A.1), that in the limit when the zonal extent of the basin becomes very large, that is, for very large $x_e - x_w$, each term *except* the first term in (A.1) remains finite. The solution of (5.8) then imposes the condition that Ψ_T must tend to zero in that limit so that, as argued heuristically in sections 3 and 4, in the unbounded case the boundary constants on the basin perimeter can (indeed must) be taken to be zero. Thus, there is a qualitative difference in the role of the boundary constants. That springing from the application of Kelvin's theorem is more local and depends only on the passage of the Kelvin wave around the island segment. The constants arising from the mass conservation condition depend on the passage of a Kelvin wave around the entire basin (or each subbasin if they are isolated). We expect the former to be a more robust phenomenon, less sensitive to dissipative and nonlinear phenomena throughout the basin.

Figure 9 shows the response for $\Delta\Psi_I$, the barotropic mass flux through the gaps, as a function of forcing frequency. Here $\kappa = 0.001$. Several peaks, corresponding to the free modes of oscillation are evident, the spatially gravest mode corresponding to the highest frequency at $\omega = 0.100\,86$. The asterisks in the figure correspond to the barotropic normal mode frequencies in the absence of the barrier (Pedlosky 1987). It is clear that the gravest mode has a somewhat reduced frequency but that the lower frequency modes correspond quite well to the barrier-free case in agreement with the earlier results in PS. Figure 10a shows the forced wave at four points in its period of oscillation. The position of the forcing is not evident because at resonance the motion is dominated by the structure of the free mode of oscillation. Figure 10b shows the absolute value of the streamfunction, that is, the membrane function ϕ_B. Figure 10 makes very clear the ability of the large-scale wave motion to squeeze through the gaps and reemerge in the eastern basin with a large-scale organized oscillation.

[1] The author is indebted to Paola Cessi for pointing this out to him.

For the baroclinic mode the nature of the solution clearly depends on the degree of stratification. For small F the wave equation (2.7b) approximates that of the barotropic mode. At the same time, the effect of the boundary term arising from the interface motion at the eastern boundaries of the two subbasins becomes negligible (note that g_{n1} goes to zero as F approaches zero). Thus, for small F the form of the solution, and the resonant frequencies of the baroclinic problem, will approach the barotropic example discussed above. The situation becomes more interesting for large F.

Figure 11 shows the response curves, also for $\kappa = 0.001$ and $F = 300$, for the two baroclinic constants arising from (5.8). The solid curve shows $\Psi_{IT} - \Psi_T$, and hence the baroclinic flux through the gaps and thus also (see 5.6b) the forcing term due to the antenna effect of the island segment, while the dashed curve shows the response of Ψ_T, which measures the forcing due to the eastern boundary radiation in each basin set up by the baroclinic Kelvin wave that has circumnavigated the entire basin. We note in the figure that this second effect, as measured by the relative size of two terms, is small compared to the antenna effect. Note also that, because of the much lower frequencies involved for the baroclinic modes, the resonant peaks, while still evident, are much less sharp than for the barotropic mode. Figure 12a shows the membrane function, or equivalently, the absolute value of ψ_T at the frequency with the greatest response to localized forcing in the eastern subbasin while Fig. 12b shows the response to *only* that portion of the motion due to the eastern boundary term, that is, the portion proportional to Ψ_T. Note, that this second part has a much larger meridional scale, essentially the scale of the basin since it is forced by the entire length of the eastern boundaries of the subbasins while the full mode has a scale that reflects more clearly the meridional scale of the island segment.

b. Partial gaps

The problem that arises when the basin is closed and the gaps in the barrier exist only in the upper layer is the most complex of all the examples. In this case there are three constants to be determined (Ψ_{I1}, Ψ_2^R, Ψ_2^L) and as opposed to the full gap case, since the barotropic and baroclinic modes are coupled, the constraints relating these three constants are also coupled. The solutions to localized forcing in the eastern subbasin (again a delta function at $x = z$), is for the barotropic mode for $x > x_t$, (and suppressing the exponential time factor)

$$\psi_B = h_2\Psi_2^R + \sum_n \sin n\pi y\left\{h_1\Psi_{I1}g_{n2}\frac{\sin a_n(x - x_e)}{\sin a_n(x_t - x_e)}e^{ik(x-x_t)} - \frac{2ikw_{Bn}}{a_n}\frac{e^{ik(x-z)}}{\sin a_n(x_t - x_e)}\right.$$
$$\left.\times[\Theta(x-z)\sin a_n(x_t - z)\sin a_n(x - x_e) + \Theta(z-x)\sin a_n(x_t - x)\sin a_n(z - x_e)]\right\}, \quad (5.9a)$$

while for $x < x_t$,

$$\psi_B = h_2\Psi_2^L + \sum_n \sin n\pi y\left\{h_1\Psi_{I1}g_{n2}\frac{\sin a_n(x - x_w)}{\sin a_n(x_t - x_w)}e^{ik(x-x_t)}\right\}. \quad (5.9b)$$

Similarly, for the baroclinic mode, for $x > x_t$,

$$\psi_T = -\Psi_2^R\frac{\cosh\lambda(y - 1/2)}{\cosh\lambda/2} + \sum_n \frac{\sin n\pi y}{\sin b_n(x_t - x_e)}$$
$$\times\left\{\Psi_{I1}g_{n2}\sin b_n(x - x_e)e^{ik(x-x_t)} - \Psi_2^R g_{n1}[\sin b_n(x - x_e)e^{ik(x-x_t)} - \sin b_n(x - x_t)e^{ik(x-x_e)}]\right.$$
$$\left.-\frac{2ikw_{Tn}}{b_n}e^{ik(x-z)}[\Theta(x-z)\sin b_n(x - x_e)\sin b_n(x_t - z) + \Theta(z-x)\sin b_n(x_t - x)\sin b_n(z - x_e)]\right\}, \quad (5.9c)$$

while for the baroclinic solution in the western subbasin ($x < x_t$),

$$\psi_T = -\Psi_2^L\frac{\cosh\lambda(y - 1/2)}{\cosh\lambda/2} + \sum_n \frac{\sin n\pi y}{\sin b_n(x_t - x_w)}$$
$$\times\{\Psi_{I1}g_{n2}\sin b_n(x - x_w)e^{ik(x-x_t)} - \Psi_2^L g_{n1}[\sin b_n(x - x_w)e^{ik(x-x_t)} - \sin b_n(x - x_t)e^{ik(x-x_w)}]\}. \quad (5.9d)$$

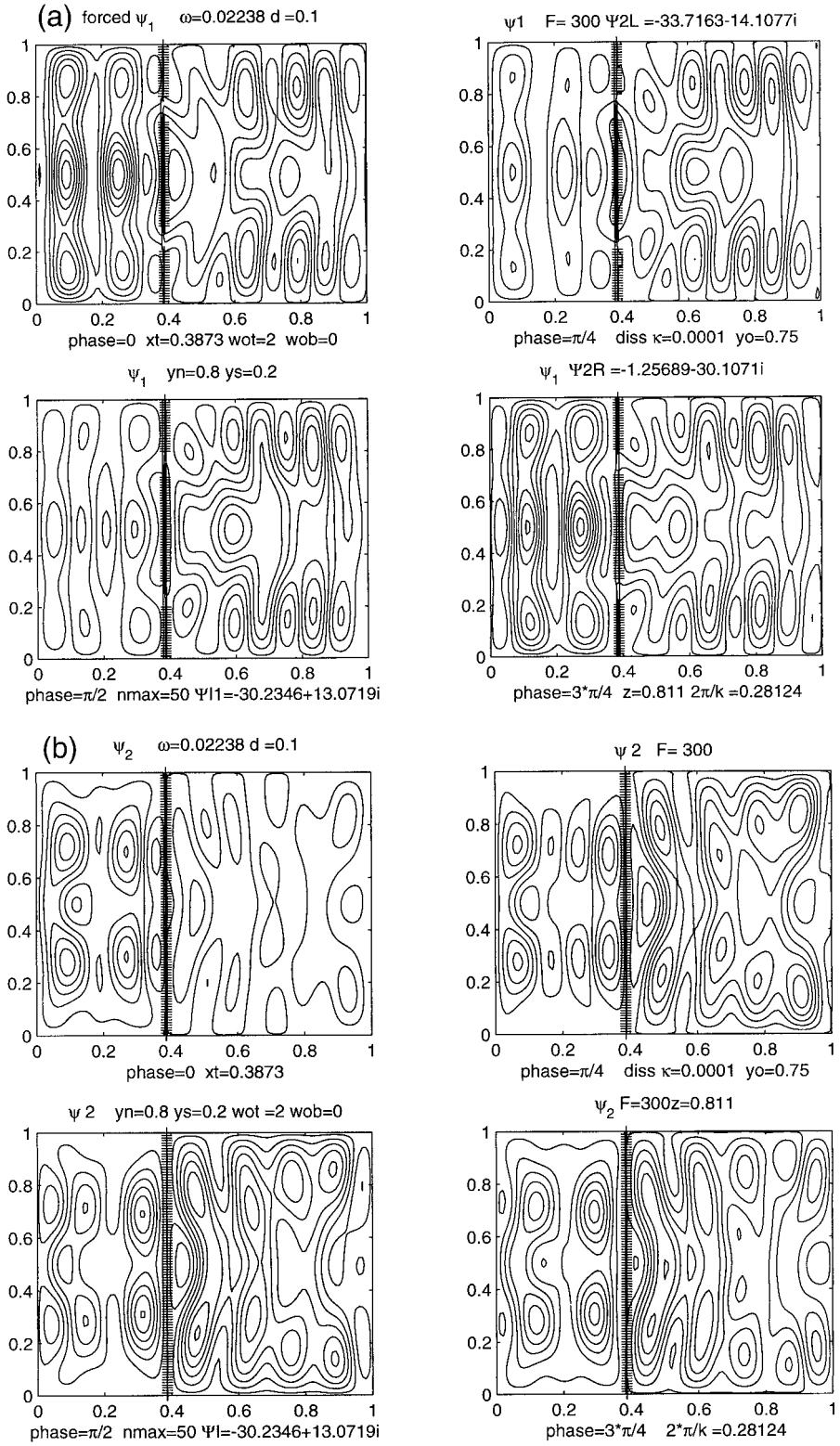

FIG. 16. The wave response for the parameters of Fig. 15 at the frequency $\omega = 0.022\,38$: (a) the upper-layer solution at four instants in the wave period, (b) the lower layer at those same times, (c) the absolute value of the barotropic streamfunction, and (d) the absolute value of the baroclinic field.

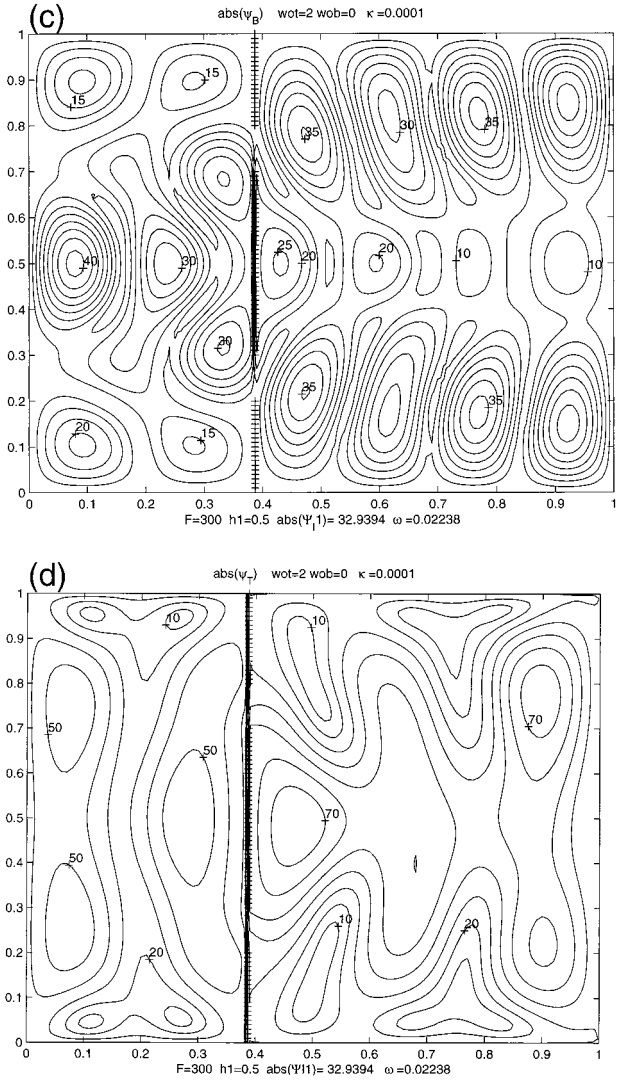

FIG. 16. (*Continued*)

To complete the solution the three boundary constants must be determined. As described in section 2 the constants are determined in this case by the conditions: 1) the circulation condition applied to the upper layer where the island segment forms an island, 2) the mass conservation constraint for the eastern subbasin in the lower layer, and 3) the same conservation constraint for the western subbasin. These three constraints lead to three coupled equations for Ψ_{I1}, Ψ_2^R, Ψ_2^L, which can be put in the form

$$A_1\Psi_2^L + A_2\Psi_2^R + A_3\Psi_{I1} = Y_1, \qquad (5.10a)$$

$$B_1\Psi_2^L + B_2\Psi_{I1} = 0, \qquad (5.10b)$$

$$D_1\Psi_2^L + D_2\Psi_{I1} = Y_2. \qquad (5.10c)$$

The coefficients of these three equations for Ψ_{I1}, Ψ_2^R, Ψ_2^L are given in appendix B.

Because of the possibility of resonance there are a great number of interesting examples that could be investigated with this solution. However, since the focus of this paper is not on the normal modes but on the transmission and transformational properties of the Rossby waves due to the gappy barrier, we will consider only two examples of the partial gap case in detail. In both cases the forcing is purely baroclinic, representing an imposed potential vorticity source with no vertical mean. To recall, this would be the property of a pv eddy flux due to midocean baroclinic eddy activity. Other forcings could be easily considered, but the main points can be illustrated most simply with this forcing. If F is very small, the transmission will be limited to only the upper layer and the transmission problem reduces to the problem for a single layer. The more interesting case occurs when the deformation radius is small with respect to the basin scale. Hence, as before, we consider the case where $F = 300$.

Consider first the case where the PV damping timescale is of the same order as the baroclinic wave period. Figure 13 shows the response curve for the three constants Ψ_{I1}, Ψ_2^R, Ψ_2^L as a function of frequency for $F = 300$ and for $\kappa = 0.01$. There is a broad peak near $\omega = 0.02$. The solid curve gives the response for Ψ_{I1}, the dashed curve gives the boundary constant for the eastern subbasin Ψ_2^R, while the dotted curve gives the boundary constant for the western subbasin Ψ_2^L. Note that the transmitted wave depends on the first and last of these and of the two, it is the island constant, measuring the gap flux in the upper layer and the strength of the island segments radiation, that is dominant. This is consistent with our earlier discussion, relative to Fig. 11, about the greater robustness of the antenna effect compared with the mass conservation constraint with respect to dissipation in the wave field.

Figure 14 shows the wave field response for forcing at the frequency $\omega = 0.02$. Figure 14a shows the upper-layer streamfunction at four instants during the wave period. Figure 14b shows the same for the lower layer while Figs. 14c and 14d show the barotropic and baroclinic wave fields. It seem evident from the structure of the wave fields in the western basin that the antenna mechanism associated with the gaps is important for the wave transmission in the upper layer. It is less clear for the lower layer as shown in Fig. 14b. For this fairly dissipative case, where the ratio of ω to κ is $O(1)$, we observe a strong western intensification of the wave signal in the western subbasin. Again, as in the free wave case, although the forcing is purely baroclinic, it is evident from Fig. 14c that the steep topography represented by the barrier is a source of barotropic wave radiation, strongly limited to the east of the barrier to a narrow zonal region while extending westward over the whole western subbasin. Figure 14d shows contours of the baroclinic part of the flow. Note that most of the baroclinic amplitude is centered on the forcing region; only a relatively small fraction is transmitted. However, the amplitude of the transmitted baroclinic, while almost

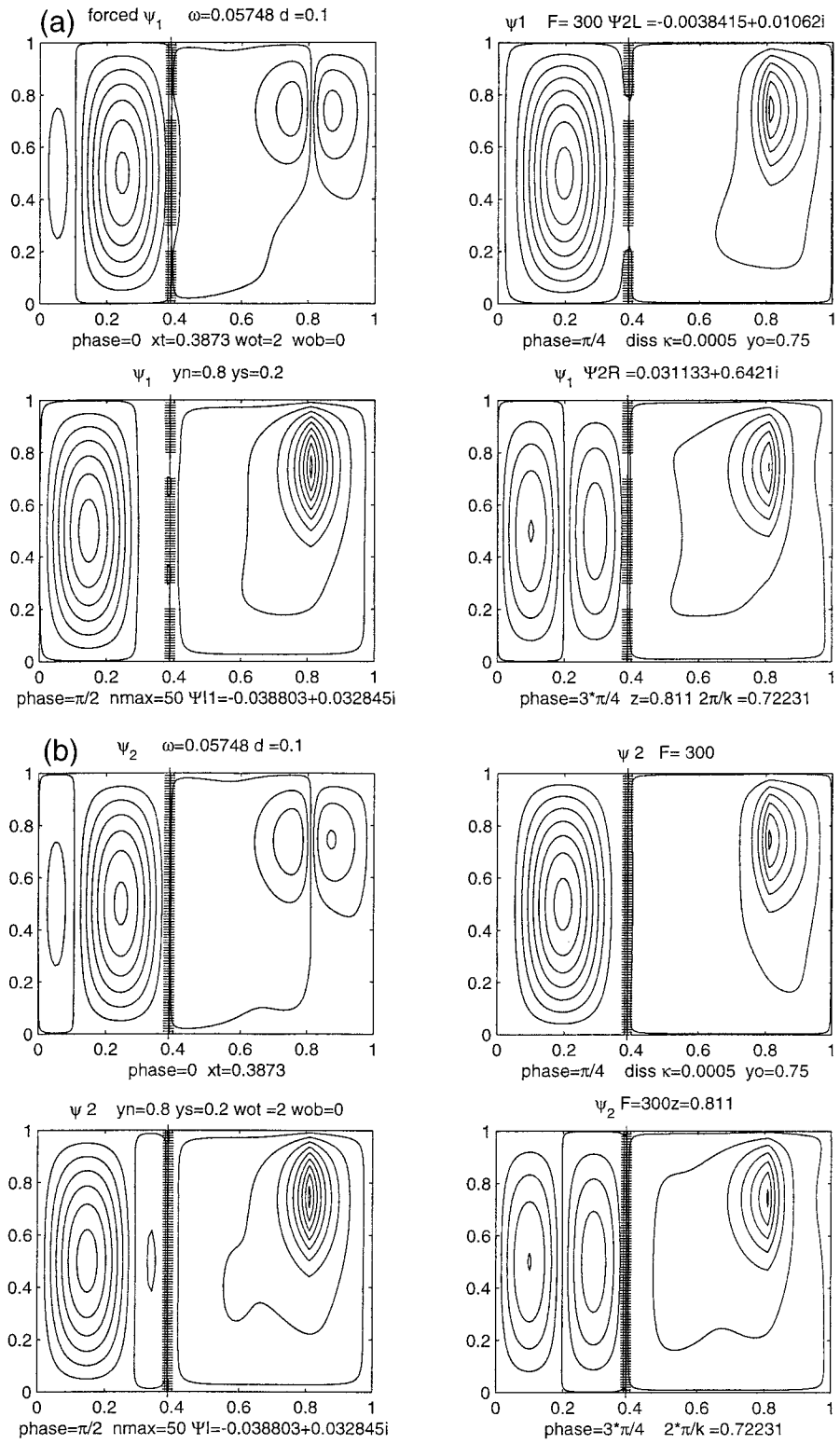

FIG. 17. The wave response for purely baroclinic forcing at a frequency $\omega = 0.057\,48$ corresponding to the first barotropic normal mode of the western subbasin; $F = 300$ and $\kappa = 0.0005$: (a) the streamfunction in the upper layer, (b) the lower layer, (c) the absolute value of the barotropic streamfunction, and (d) the absolute value of the baroclinic streamfunction.

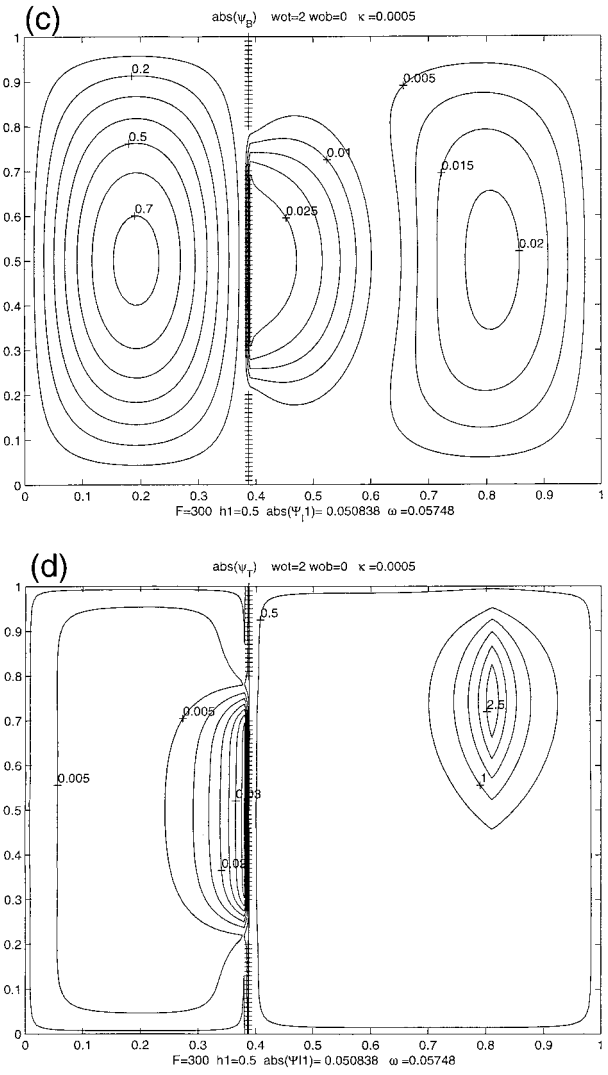

FIG. 17. (*Continued*)

everywhere smaller than the barotropic wave amplitude in the western subbasin, is of roughly the same order.

At smaller levels of dissipation the normal mode character of the response becomes more evident. Figure 15 shows the response for Ψ_{I1}, Ψ_2^R, Ψ_2^L when $\kappa = 0.0001$ and $F = 300$. The figure is displayed in panels. The major peak occurs at $\omega \approx 0.0228$ while the remaining peaks at higher frequency have much smaller amplitudes for all three constants. So as to allow all the peaks to be easily seen, the frequency interval has been split into two intervals. The peaks at higher frequency actually correspond to resonances with the barotropic subbasin modes with $n = 1$ for the eastern subbasin. Although there is enough flow through the gaps and around the island segment to satisfy Kelvin's theorem, there is relatively little transmission of wave energy from the eastern to the western basin at these frequencies compared to the resonant pileup of energy that remains in the east. At lower frequencies, especially at the peak seen in Fig. 15a at $\omega \approx 0.022\,38$, the wave mode involves both subbasins equally. The response is shown in Fig. 16. The upper- and lower-layer response is shown in Figs. 16a,b. In this case as seen in Figs. 16c and 16d the baroclinic and barotropic responses in the western subbasin are of the same order. The dissipation is so low that the barotropic field, produced by reflection from the topographic barrier, is able to radiate eastward and fill the eastern basin rather than be limited to a narrow zone near the barrier. The near equivalence of barotropic and baroclinic amplitude in the western basin is signaled by the response curve in Fig. 15a, where it is seen that the gap flux term Ψ_{I1} is actually slightly smaller than the boundary perimeter term Ψ_2^L. This is the only example of this that has appeared and seems limited to the low dissipation limit.

An interesting and rather bizarre example, but one that demonstrates the transformational ability of the barrier, is shown in Fig. 17. In this case, again for $F = 300$ and for $\kappa = 0.0005$, the frequency of the PV source has been chosen to be the resonant frequency for the first barotropic mode of the western subbasin. The forcing however, is purely baroclinic. Figures 17a and 17b, show the wave field during the oscillation. In the eastern subbasin the response is limited to the forcing region. In the western subbasin an ordinary Rossby basin mode is excited by relatively weak flow through the gaps. Figures 17c and 17d show the barotropic and baroclinic wave amplitudes, and it is clear from the contour magnitudes that the baroclinic motion is strongly focused around the source and due to the resonance the western subbasin is entirely dominated by the *barotropic* mode. Of course, at higher dissipation, where the reflections are damped this resonance becomes very weak.

6. Discussion

A series of examples of increasing complexity has been considered for the problem of the transmission of Rossby waves through leaky barriers, representing steep topography with gaps or an extensive island arc chain. The constraint imposed by Kelvin's theorem allows a surprisingly easy passage of wave energy through the barrier as long as more that one gap in the barrier is present.

In the presence of stratification the nature of the transmission depends very strongly on the degree to which the gaps in the barrier are complete, that is, span the full depth of the fluid or if the gaps are only partial so that the deeper layers are completely blocked. In the latter case, the problem sequence involving free and forced Rossby waves, with and without basin resonance, shows the basic transformational character of the topography. In particular, motion that originally radiates westward primarily in the baroclinic mode of our two-layer model is transformed into barotropic wave energy by its interaction with the barrier. It is important to note that the transmission does not depend on the existence

of full basin modes but occurs whenever any large-scale wave is incident on the barrier. Indeed, unless the dissipation is very small, and resonance takes place, the transformation is abrupt in the sense that the resulting barotropic motion is essentially limited to the western subbasin.

The barrier has been introduced in these examples as a highly simplified representation of steep topography like the midocean ridge or the incomplete barriers of island arc systems. In particular, the transformation of the vertical structure at the barrier recalls the observations of Chelton and Shlax (1996) alluded to in the introduction in which altimeter data seems to show the production of low mode (in their case first baroclinic mode) energy propagating westward from the midocean ridge in the North Pacific. Of course, our model is really too simple to adequately model the situation to which the observations are pertinent. A more complex 2½-layer model would be more relevant. However, the added analytical complexity of an additional interface and an additional mass conservation condition speaks against considering such a model as a first step. Nevertheless, with the results of the present model in mind we might speculate that the barotropic mode of the two-layer model considered here is analogous to the first baroclinic mode of the reduced gravity model and our baroclinic mode would model higher baroclinic modes in the reduced gravity model. If that were so, it is tempting to speculate that internal higher baroclinic processes, of second-mode type, produced by internal instability processes, if radiated westward, would be transformed to a low-mode structure and be more readily observed in the altimeter data west of the midocean ridge.

In addition to the idealization of the two-layer model in terms of vertical structure, the use of linear theory and the absence of the interactions with mean currents substantially weakens our ability to make direct comparison between the results of this model and the observations. However, the simplicity of the Kelvin constraint and the robustness of the transformation properties due to the topography make it plausible that the process will reappear in more realistic models even if quantitatively distorted by these additional effects.

Acknowledgments. This research was supported in part by a grant from the National Science Foundation, OCE 9901654. Helpful conversations with Mike Spall and Paola Cessi are gratefully acknowledged.

APPENDIX A

Coefficients for the Boundary Constants in (5.8)

Application of the mass conservation theorem, that is, setting the integral of the baroclinic streamfunction over the full basin equal to zero yields as coefficients in (5.8a):

$$C_1 = (x_e - x_w)\frac{2}{\lambda}\tanh\lambda/2 - \sum_n \frac{2\mu_n g_{n1} b_n}{n\pi(n^2\pi^2 + F)}\left[\frac{\sin b_n(x_e - x_w)}{\sin b_n(x_t - x_w)} + \frac{\cos k(x_w - x_t)}{\sin b_n(x_t - x_w)} - \frac{\cos k(x_e - x_t)}{\sin b_n(x_t - x_e)}\right],$$

$$C_2 = -\sum_n \frac{\mu_n g_{n2} b_n}{n\pi(n^2\pi^2 + F)}\left\{\frac{\sin b_n(x_e - x_w)}{\sin b_n(x_t - x_w)\sin b_n(x_t - x_e)} + \frac{e^{ik(x_w - x_t)}}{\sin b_n(x_t - x_w)} - \frac{e^{ik(x_e - x_t)}}{\sin b_n(x_t - x_e)}\right\},$$

$$X_1 = \sum \frac{2k\mu_n w_{Tn}}{in\pi(n^2\pi^2 + F)}\left[1 - \frac{\sin b_n(x_t - z)}{\sin b_n(x_t - x_e)}e^{ik(x_e - z)} - \frac{\sin b_n(z - x_e)}{\sin b_n(x_t - x_e)}e^{ik(x_t - z)}\right]. \quad \text{(A.1)}$$

The application of Kelvin's theorem yields the coefficients in (5.8b), namely

$$C_3 = \sum_n b_n g_{n3} g_{n1}\left[\frac{\sin b_n(x_e - x_w)}{\sin b_n(x_t - x_e)\sin b_n(x_t - x_w)} - \frac{e^{-ik(x_e - x_t)}}{\sin b_n(x_t - x_e)} + \frac{e^{ik(x_w - x_t)}}{\sin b_n(x_t - x_w)}\right],$$

$$C_4 = \sum_n b_n g_{n3} g_{n2}\frac{\sin b_n(x_e - x_w)}{\sin b_n(x_t - x_e)\sin b_n(x_t - x_w)},$$

$$X_2 = -e^{-ik(z - x_t)}\sum_n 2ikw_{Tn}g_{n3}\frac{\sin b_n(z - x_e)}{\sin b_n(x_t - x_e)}. \quad \text{(A.2)}$$

APPENDIX B

Coefficients of Boundary Constants in (5.10)

As described in the text, the application of Kelvin's theorem around the island segment in the upper layer and the two mass conservation conditions for the two subbasins formed by the lower layer in the partial gap case, leads to (5.10a,b,c). Using the solution in (5.9) we obtain, as coefficients in (5.10), the following. From the circulation condition,

$$A_1 = h_2\sum_n g_{n1}g_{n3}[ik + b_n\{\cot b_n(x_t - x_w) - e^{ik(x_w - x_t)}/\sin b_n(x_t - x_w)\}], \quad \text{(B.1a)}$$

$$A_2 = -h_2 \sum_n g_{n1} g_{n3} [ik + b_n \{\cot b_n(x_t - x_e) - e^{ik(x_t - x_e)}/\sin b_n(x_t - x_e)\}], \tag{B.1b}$$

$$A_3 = \sum_n g_{n2} g_{n3} \left[\frac{h_1 a_n \sin a_n(x_e - x_w)}{\sin a_n(x_t - x_e) \sin a_n(x_t - x_w)} + \frac{h_2 b_n \sin b_n(x_e - x_w)}{\sin b_n(x_t - x_e) \sin b_n(x_t - x_w)} \right]. \tag{B.1c}$$

From the mass conservation condition in the western subbasin,

$$B_1 = -(x_t - x_w)\frac{2}{\lambda} \tanh\lambda/2 + 2 \sum_n \frac{\mu_n g_{n1} b_n}{n\pi(n^2\pi^2 + F)} \times \left[\frac{\cos k(x_w - x_t)}{\sin b_n(x_t - x_w)} - \cot b_n(x_t - x_w) \right], \tag{B.2a}$$

$$B_2 = -\sum_n \frac{\mu_n g_{n2}}{n\pi(n^2\pi^2 + F)} \times \left[ik - b_n \cot b_n(x_t - x_w) + \frac{b_n e^{ik(x_w - x_t)}}{\sin b_n(x_t - x_w)} \right], \tag{B.2b}$$

while from the mass conservation integral for the eastern subbasin,

$$D_1 = -(x_e - x_t)\frac{2}{\lambda} \tanh\lambda/2 + 2 \sum_n \frac{\mu_n g_{n1} b_n}{n\pi(n^2\pi^2 + F)} \times \left[\cot b_n(x_t - x_e) - \frac{\cos k(x_e - x_t)}{\sin b_n(x_t - x_e)} \right], \tag{B.3a}$$

$$D_2 = -\sum_n \frac{\mu_n g_{n1}}{n\pi(n^2\pi^2 + F)} \times \left[-ik + b_n \cot b_n(x_t - x_w) - b_n \frac{e^{ik(x_e - x_t)}}{\sin b_n(x_t - x_e)} \right], \tag{B.3b}$$

$$Y_2 = \sum \frac{2k\mu_n w_{Tn}}{in\pi(n^2\pi^2 + F)} \left[1 - \frac{\sin b_n(x_t - z)}{\sin b_n(x_t - x_e)} e^{ik(x_e - z)} - \frac{\sin b_n(z - x_e)}{\sin b_n(x_t - x_e)} e^{ik(x_t - z)} \right]. \tag{B.3c}$$

REFERENCES

Barnier, B., 1984: Influence of a mid-ocean ridge on wind driven barotropic ocean waves. *J. Phys. Oceanogr.*, **14,** 1930–1936.

Chelton, D. B., and M. G. Schlax, 1996: Global observations of oceanic Rossby waves. *Science*, **272,** 234–238.

Edwards, C. A., and J. Pedlosky, 1995: The influence of distributed sources and upwelling on the baroclinic structure of the abyssal circulation. *J. Phys. Oceanogr.*, **25,** 2259–2284.

Flierl, G. R., 1977: Simple applications of McWilliams ''A note on a consistent quasi-geostrophic model in a multiply connected domain.'' *Dyn. Atmos. Oceans*, **5,** 443–454.

Kawase, M., 1987: Establishment of deep ocean circulation driven by deep-water formation. *J. Phys. Oceanogr.*, **17,** 2294–2317.

Matano, R. P., 1995: Numerical experiments on the effects of a meridional ridge on the transmission of energy by barotropic Rossby waves. *J. Geophys. Res.*, **100** (C9), 18 271–18 280.

McKee, W. D., 1972: Scattering of Rossby waves by partial barriers. *Geophys. Fluid Dyn.*, **4,** 83–89.

McWilliams, J. C., 1977: A note on a consistent quasi-geostrophic model in a multiply connected domain. *Dyn. Atmos. Oceans*, **5,** 427–442.

Pedlosky, J., 1987: *Geophysical Fluid Dynamics*. Springer Verlag, 710 pp.

——, and M. Spall, 1999: Rossby normal modes in basins with barriers. *J. Phys. Oceanogr.*, **29,** 2332–2349.

Wang, L., and C. J. Koblinsky, 1994: Influence of mid-ocean ridges on Rossby waves. *J. Geophys. Res.*, **99** (C12), 25 143–25 153.

Zang, X., and C. Wunsch, 1999: The observed dispersion relation for North Pacific Rossby wave motions. *J. Phys. Oceanogr.*, **29,** 2183–2190.